Screening Model for CO_2 Miscible Flooding

by

Kuhaneswaren A/L Ramah Moorthy

Dissertation submitted in partial fulfillment of
the requirement for the
Bachelor of Engineering (Hons)
(Mechanical Engineering)

SEPTEMBER 2012

Universiti Teknologi PETRONAS
Bandar Seri Iskandar
31750 Tronoh
Perak Darul Ridzuan

CERTIFICATION OF APPROVAL

Screening Model for CO_2 Miscible Flooding

by

Kuhaneswaren Ramah Moorthy

A project dissertation submitted to the
Mechanical Engineering Programme
Universiti Teknologi PETRONAS
in partial fulfilment of the requirement for the
BACHELOR OF ENGINEERING (Hons)
(MECHANICAL ENGINEERING)

Approved by,

_____

(Dr.William Pao King Soon)

UNIVERSITI TEKNOLOGI PETRONAS

TRONOH, PERAK

September 2012

CERTIFICATION OF ORIGINALITY

This is to certify that I am responsible for the work submitted in this project, that the original work is my own except as specified in the references and acknowledgements, and that the original work contained herein have not been undertaken or done by unspecified sources or persons.

_____

KUHANESWAREN A/L RAMAH MOORTHY

Table of Contents

List of Figures

ABSTRACT

CO_2 MIST (Carbon Dioxide Miscible Flooding Screening Tool) is designed to provide an inexpensive and reliable method in screening carbon dioxide flooding (CO_2). CO_2 flooding can be considered one of the methods which offer the potential of additional oil recovery. The parameters and key factors that help in mobilizing reservoir oil and influence the whole process of CO_2 flooding are discussed. These parameters are recognized and thus are converted into a screening tool using Excel-VBA that would help enable proper reservoir modeling of the whole process. Key points in the choice of miscible flooding are also described in this report by portraying its advantages. The model would then be further analyzed and compared to field data so that the program will be deemed suitable for practical and field use.

CHAPTER 1 INTRODUCTION

1.1 Background of Study

Global concerns on green house gas emissions into the environment have prompted interest in carbon dioxide capture and sequestration (CCS). One such method described by McCoy et al. (2006) of sequestering carbon dioxide would be through CO_2 flood-enhanced oil recovery (CO_2-EOR).

Enhanced oil recovery through CO_2 flooding can increase oil production in the final stages of a reservoir's life where CO_2 has the ability to enter zones that were not previously invaded by water. This causes trapped oil to be released and at the same time a fraction of CO_2 is trapped underground (Andrei *et al*., 2011).

The process of CO_2 flooding can be divided into two main mechanisms which would be miscible and immiscible processes (Shah, 2008). In miscible flooding the suitable reservoir conditions are those that are below 1200 meters and oil density is above 22^o API. The CO_2 injected into the reservoir does not completely mix with the oil, thus decreasing the interfacial tension between the substances to almost zero (from 2-3 N/m^2) and forms a low viscosity fluid that can be easily displaced. For immiscible flood, it is used when reservoir pressure is too low and the oil density is too high. The CO_2 injected to not mix with the oil within the reservoir but alternatively causes the swelling of the oil, resulting in a reduction in density, improving its mobility and thus increases the oil recovery (Andrei *et al*., 2011).

1.2 Problem Statement

Taking into view, the significant effects of CO_2 miscible flooding towards enhanced oil recovery and its environmental contributions, an extensive, inexpensive and reliable method for screening CO2 miscible flooding is proposed in this study.

1.2.1 Significance of project

The model encompasses a simplified reservoir model for the prediction of CO_2 rates and the associated enhanced fossil fuel recovery. The screening model predicts the feasibility of the flood campaign and its performance given the known reservoir parameters. It is intended to be used as an integrated add-on toolkit, providing the engineers and decision makers a simple "back of the envelope" calculation platform.

1.3 Objectives

There are several objectives that need to be achieved when completing this project. The objectives are:

1. Identifying parameters and key factors that influence CO_2 flooding.
2. Develop and implement the CO_2 flow model based on the fractional flow theory, modified for the effects of viscous fingering, vertical heterogeneity and gravity segregation.
3. Demonstrating using field data and test cases and the associated parametric studies.
4. Workflow integration into a deployable and user friendly package.

1.3.1 Scope of Study

The research will involve the understanding of the fractional flow theory which is modified to accommodate the effects of viscous fingering, vertical heterogeneity and gravity segregation. The Simple Wave Theory is also incorporated in the research, where the Koval Factor is used for the study of viscous fingering and the Dystra Parsons coefficient is used for Reservoir Heterogeneity. The study of this project can be broken down to the identification of appropriate parameters and key factors that influence CO_2 flooding and thus integrating them into a single screening model.

1.4 Relevance of the Study

This project focused on the topic of fractional flow of CO_2 and reservoir modeling. These topics are related to the course of Fundamentals of Reservoir Engineering and the chapter of Immiscible Displacement and the knowledge of Fluid Mechanics is needed to perform research for this project.

Being a project that is based on Enhanced Oil Recovery (EOR), focus would be placed on completing a screening model that would provide better understanding on the topic of CO_2 miscible flooding and at the same time compute a series of calculations in determining the feasibility of a project. In the screening tool oil rate versus time function is computed based on reservoir data keyed in by the user. The study offers a simplified method in screening CO_2 miscible flooding that provides substantial data on the oil recovery potential.

CHAPTER 2 LITERATURE REVIEW

This chapter described the fundamentals of CO_2 miscible flooding. Theories that have played a significant role in the study are also discussed.

2.1 CO_2 Characteristics

At normal atmospheric conditions, CO_2 is a thermodynamically stable gas that is heavier than air. Figure 2.1 would be the phase diagram of carbon dioxide:

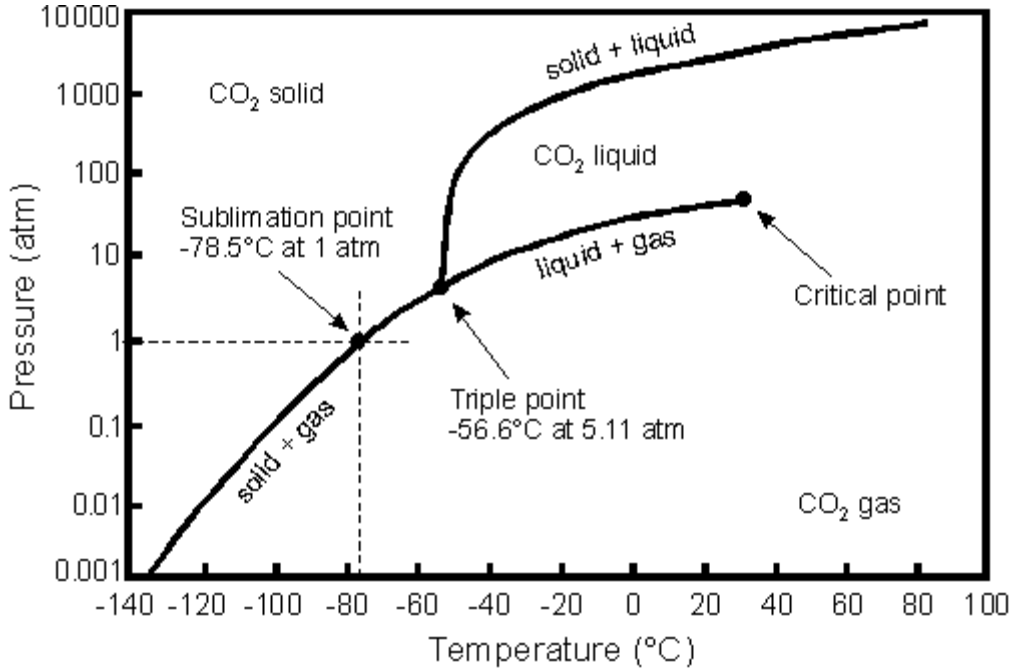

Pressure-Temperature phase diagram for CO_2.

Figure 2.1 -- Phase Diagram of CO2. Basbug et al., (2005)

Referring to the Fig. 2.1, pure carbon dioxide has a critical temperature of 31^{o}C and a critical pressure of 73 atm or 7.38 MPa. Below this temperature or pressure, the CO_2 is either in liquid or vapor phase and if above the critical values, CO_2 is in its supercritical state. The behavior of CO_2 at these temperature and pressure conditions would still remain gas-like but has a liquid density that increases, which depends on the pressure and temperature from 200 to 900 kg/m^3 (Basbug et al., 2005).

CO_2 is a water soluble gas whereby its solubility increases with pressure and decreases with temperature and water salinity. Supercritical CO_2 is immiscible in water. Solid hydrates that are heavier than water are formed at low temperatures and elevated pressures.

The gas also has a high affinity to coal whereby it is almost twice as high as methane, a gas that is abundantly found in coal beds (Basbug et al., 2005).

In terms of carbon dioxide flooding the gas generally develops miscibility with the reservoir oils through mass transfer of components (Henry & Metcalfe, 1983). In miscible flooding, it is important to measure the minimum miscibility pressure (MMP) of CO_2. Two key factors which greatly influence the CO_2 MMP would be the reservoir oil composition and temperature (Yongmao et al., 2004). Yongmao et al.,(2004) have studied the PVT properties for reservoir fluid to CO_2 mixtures where CO_2 at a concentration range from 25.20% to 62.83 mol % was combined with a reconstituted reservoir fluid.

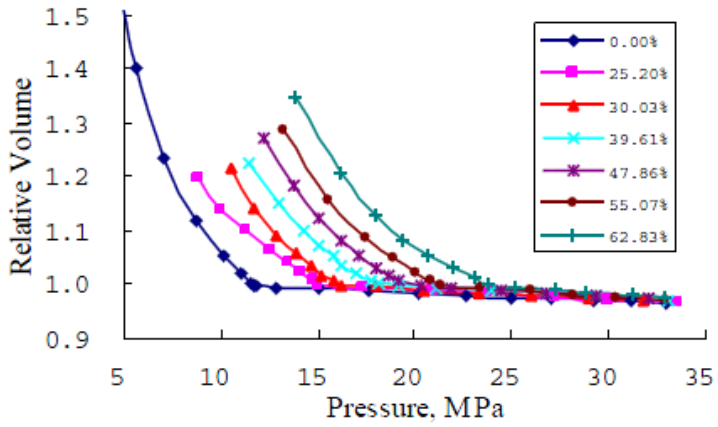

Figure 2.2 -- P-V Curves with CO_2 Concentration. Yongmao et.al (2004)

Figure 1.2 shows the P-V curves with seven different CO_2 concentrations. When the CO_2 concentration is lower there is a clear inflexion on each curve,meaning that gas phase appears at the inflexion and the pressure at that point would be the bubble point pressure. When the CO_2 concentration reaches a mol percentage of 62.83, the bubble point cannot be directly determined from the P-V curve and it can be deduced that the reservoir fluid and CO_2 has reached the one-contact miscible state at that CO_2 concentration (Yongmao et al., 2004). The bubble point is the pressure and temperature conditions at which the first bubble of gas comes out of a solution of oil.

At a given temperature in the reservoir, the pressure maybe sufficiently high to keep all the existing gases in the solution. However, as the pressure is reduced by production after flooding, the system will eventually reach the bubble point pressure of either oil or water (Vetter et al., 1987). As soon as bubble point pressure is reached in a three-phase system, the gases will start to flash and as the pressure is further reduced, the thermodynamic variables of

both oil and water will start to change. Reactive gases such as CO_2 which are mutually soluble in the liquid oil and water phases would change the chemical behaviour.

2.3 CO_2 Miscible Flooding

There are three notable techniques for oil recovery which would be the primary, secondary and the tertiary recovery operation (Andrei et al., 2011). Primary and secondary methods together recover close to 21% of the original oil in place (OOP) (Srivastava & Huang, 1997). Enhanced Oil Recovery which is promoted by CO_2 flooding comes into tertiary recovery operations where it is applicable to oilfields that are approaching their end of life and are able to produce additional oil in the range of 5-15% of OOP for light to medium oil rated according to the API standard. The recovery rate is lower for heavy oil reservoirs for oil below 20^o degree API (Andrei et al., 2011). Some positives of CO2 floods compared to other conventional methods would be that it helps minimize gravity segregation compared to hydrocarbon solvents and it generally costs less (Srivastava & Huang, 1997).

CO_2 is not miscible with reservoir oil at first contact. Hence, this is where miscible flooding is brought into play. Reservoirs with pressures at or beyond Minimum Miscibility Pressure (MMP) to the injected stream of CO_2 promote multiple contact miscibility (Asghari & Dong, 2007). Hence, the ability to achieve dynamic miscibility at normal reservoir pressures in a wide range of reservoir types in different areas is a major advantage of the CO_2 miscible process.

Miscibility pressures are affected by several factors such as CO_2 purity, reservoir temperature and oil composition (Stalkup, 1978). Stalkup (1978) also stated that a relatively small amount of methane or nitrogen gas in CO_2 would be able to increase the pressure for miscibility

Listed below would be the advantages of a CO_2-Flood (Stalkup, 1983). :

- Miscibility of CO_2- Reservoir Oil can be achieved at relatively low pressures
- The recovery of oil is enhanced using a solution-gas drive
- Displacement efficiency is high in miscible cases
- Miscibility in reservoir can be regenerated if lost

The CO_2 miscible displacement process is shown in Fig. 2.3 below.

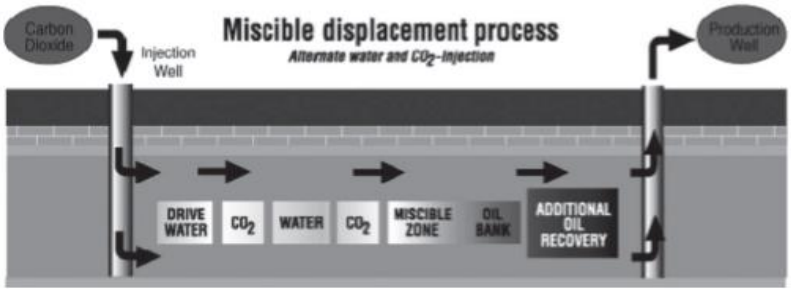

Figure 2.3 -- Miscible CO_2 Flood. Stalkup(1983)

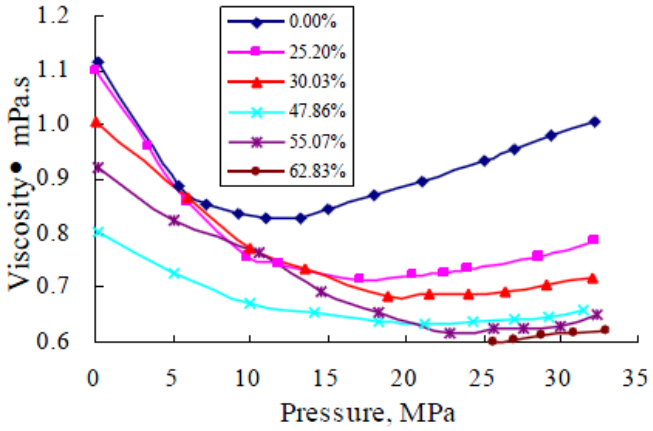

Figure 2.4 -- Viscosity as a Function of Pressure. Yongmao et.al (2004)

The reduction in viscosity of oil is an important factor in CO_2 miscible flooding. From Fig. 2.4 it can be seen that injection of CO_2 can lower the oil viscosity from 0.89 mPa.s to 0.60 mPa.s. Statistical data have indicated that 10%-70% of viscosity can be lowered using CO_2 injection (Yongmao et al., 2004).

2.4 CO_2 Flooding Process and Tools Required

In theory, the minimum data required to exercise the reservoir model as stated by Paul et al. (1984) would be permeability, depth, porosity, reservoir pressure, API gravity and pay thickness. On the basis of the simulation model, the fractional flow theory plays a major part in the development and understanding of the program.

The fractional flow-theory is a one dimensional solution by the method of characteristics (MOC) which was initially developed by Helfferich (1981). The fractional flow equation that

would be referred to would be the Buckley-Leverett model. According to the Buckley-Leverett model (Buckley & Leverett, 1942; Norman, 2001; Kleppe, 2011), the theory maintains that mass is conserved and a mass balance equation is formed. The Buckley-Leverett equation can be written as follows for 2-phase flow:

$$\frac{\delta S_w}{\delta t} + \frac{q}{A\emptyset}\frac{\partial f_w}{\partial X} = 0 \tag{1}$$

$$\frac{\delta S_g}{\delta t} + \frac{q}{A\emptyset}\frac{\partial f_g}{\partial X} = 0 \tag{2}$$

$$\frac{\delta S_o}{\delta t} + \frac{q}{A\emptyset}\frac{\partial f_o}{\partial X} = 0 \tag{3}$$

Since we have

$$S_w + S_o + S_g = 1 \tag{4}$$

Only two of these properties are independent. By neglecting gravity and capillarity, the fractional flows are

$$f_w = \frac{\frac{k_{rw}}{\mu_w}}{\frac{k_{rw}}{\mu_w}+\frac{k_{rg}}{\mu_g}+\frac{k_{ro}}{\mu_o}} \tag{5}$$

$$f_g = \frac{\frac{k_{rg}}{\mu_g}}{\frac{k_{rw}}{\mu_w}+\frac{k_{ro}}{\mu_o}+\frac{k_{rg}}{\mu_g}} \tag{6}$$

$$f_o = \frac{\frac{k_{ro}}{\mu_o}}{\frac{k_{rw}}{\mu_w}+\frac{k_{ro}}{\mu_o}+\frac{k_{rg}}{\mu_g}} \tag{7}$$

Eqs. (1) and (2) can be further expanded to give space and time derivatives of saturation, since $f_w = f_w(S_w, S_g)$ and $f_g = f_g(S_w, S_g)$. Deriving Eq.(1) yields

$$\frac{\delta S_w}{\delta t} + \frac{q}{A\emptyset}\left[\frac{\partial f_w}{\partial S_w}\frac{\partial S_w}{\partial X} + \frac{\partial f_w}{\partial S_g}\frac{\partial S_g}{\partial X}\right] = 0 \tag{8}$$

And deriving Eqn.(2) gives

$$\frac{\delta S_g}{\delta t} + \frac{q}{A\emptyset}\left[\frac{\partial f_g}{\partial S_w}\frac{\partial S_w}{\partial X} + \frac{\partial f_g}{\partial S_g}\frac{\partial S_g}{\partial X}\right] = 0 \tag{9}$$

Using the notation $f_{11} = \frac{\partial f_w}{\partial S_w}$, etc., and normalizing *t* and *X*,

$$\frac{\partial S_w}{\partial t_D} + f_{11}\frac{\partial S_w}{\partial X_D} + f_{12}\frac{\partial S_g}{\partial X_D} = 0 \tag{10}$$

$$\frac{\partial S_g}{\partial t_D} + f_{21}\frac{\partial S_w}{\partial X_D} + f_{22}\frac{\partial S_g}{\partial X_D} = 0 \tag{11}$$

Using the method of characteristics, the velocities for the composition paths are obtained and given by

$$v_{ci} = \frac{\partial F_i}{\partial C_i} \equiv \sigma \tag{12}$$

$$\sigma_{\underline{+}} = \left(\frac{\partial X}{\partial t}_{\underline{+}}\right) = \frac{q}{A\emptyset}\frac{1}{2}\left[f_{11}f_{22} + f_{22} \underline{+} \sqrt{(f_{11}+f_{22})^2 - 4(f_{11}-f_{12}f_{21})^2}\right] \tag{13}$$

Eq.12 shows the concentration velocity, where i = 2 is the displacement of oil , i = 3 describes a miscible solvent and i = 1, is water. *F* stands for the flux and *C* is the concentration.

With the Buckley-Leverett method, oil recovery from CO_2 flooding is calculated and the required injection volume to achieve oil recovery is estimated. Typical assumptions made are dimensional flow in a homogenous, isotropic or isothermal porous medium, at most three components are flowing, at most, two phases are flowing, the fluids are incompressible, dispersion is negligible, and a continuous injection of constant composition is injected (Pope, 1980). To calculate production the fractional flow of each fluid is calculated using Eqs. 4 to 6.

The characteristic velocities $\sigma_{\underline{+}}$ define two families of composition paths or directions which would be the fast (positive) and slow (negative) paths. The fast path generally passes through the initial conditions of the reservoir while the slow path passes through the injection conditions. This sequence of paths satisfies the initial and boundary conditions and forms the composition route. The concentration velocities in this case must decrease consistently but not continuously from the initial to injected conditions. If this condition of monotonous

decrease is not followed, shocks are brought into the equation (Paul et al., 1984). Shocks are discontinuities in any physical variable where in this case would be the concentration and fractional flows.

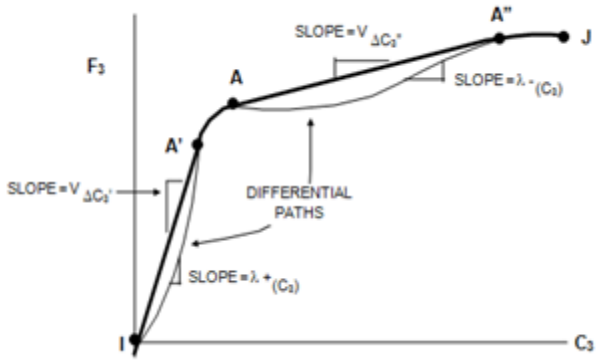

Figure 2.5 -- Flux-Concentration Plot. Paul et al (1984).

Figure 2.5 shows the flux versus concentration plot for a two phase flow that includes fast and slow paths from fractional flow. The symbol λ_{-}^{+} is equivalent to σ_{-}^{+} which is the characteristic velocity described in Eq. 12. The slope of λ^{+} shows the fast path of fractional flow whereas λ^{-} shows the slow path. Hence, shocks are introduced to eliminate any discontinuity in the flow path (Paul et al.,1984). Therefore Eq. 11, now becomes

$$v\Delta_{ci} = \frac{\Delta F_i}{\Delta C_i} \tag{14}$$

Hence, by comparing Eqs. 11 and 13, if the path calculated is close to each other the estimate of shocks are in terms with the Buckley-Leverett theory.The theory also incorporates the Koval (1963) factor that accounts for unstable miscible displacements. Taking into account the 1-D fractional flow equation, the screening tool will not be able to be used with a Koval factor that is below 1.5-2.0 where this number shows very stable miscible displacement, (Paul et al., 1986).

2.5 CO_2 Flood Design

Based on a predictive model by Paul et al., in 1986, six- section areas were identified to determine the feasibility of CO_2 flood. The evaluation was based on extensive laboratory work, reservoir simulations and also an injectivity test.

The laboratory work included black oil PVT and oil/CO_2 phase behavior studies of recombined separator oil and gas samples, CO_2 core floods and slim tube experiments. These studies were able to evaluate certain parameters such as oil swelling, phase transition pressures and viscosity reduction. The results are all taken as a function of CO_2 concentration.

Next would be the slim tube experiments, where they were utilized to determine the minimum miscibility pressure (MMP). Core floods were conducted to determine the recovery of residual oil in water and through experimentation a WAG ratio of 1:1 was deemed most efficient (Ring et al., 1995)

The injectivity test based on results taken from Ring et.al (1995), suggests that no apparent reduction in injectivity or changes in the injection profile would be apparent during or after CO_2 injection has taken place. The results were obtained by injecting a total of 31 MMscf of CO_2 (1.3% HCPV) into a well in a test period of 50 days.

The CO_2 model by Paul et al. (1986) computes CO_2 and oil recovery from the fractional flow theory that is modified to incorporate the effects of viscous fingering, areal sweep, vertical heterogeneity and gravity segregation. The theory is based on a method of characteristics known as the simple wave theory.

Hence, taking these conditions into consideration the screening tool is applicable to secondary (mobile oil present) conditions, tertiary (residual oil saturation) conditions, CO_2 slug processes, water alternating gas (WAG) processes and heterogeneous reservoirs. However there are limitations and assumptions that taken into account such as displacement of oil by CO_2 is fully miscible, the Koval factor method adequately portrays viscous fingering, the reservoir is able to take any injection rate, the CO_2 gas and water are simultaneously injected in proportion determined by a specific WAG ratio, there is no free gas saturation and the fluid properties are held constant.

2.5.1 Viscous Fingering

Viscous fingering is the process whereby viscous forces of a displacing phase have greater momentum than that of the displaced phase (Islam & Saghir, 1999). It is an important process in enhanced oil recovery and CO_2 flooding where it refers and predicts to the onset and evolution of instabilities that occur in the displacement of fluids in a porous bed. The process may come into play when a less viscous fluid that has higher mobility starts to penetrate a more viscous fluid that has lower mobility, during a displacement process.

Juanes et. al (2006), have researched on the impact of viscous fingering on the prediction of optimum WAG ratio and have come up with several governing equations that explain on how viscous fingering affects miscible flooding especially in an attempt to reduce the mobility contrast between injected and displaced fluids. The following mathematical model describes one dimensional flow, while ignoring the effects of viscous fingering.

$$\frac{\partial S}{\partial t} + \frac{\partial f}{\partial x} = 0 \tag{15}$$

$$\frac{\partial C}{\partial t} + \frac{\partial}{\partial x}\left((1-f)\frac{C}{1-S}\right) = 0 \tag{16}$$

Both the Eqs. 15 and 16 are from the Buckley-Leverett equation, where *S* stands for the water saturation, f denotes the water fractional flow and both *x* and *t* are dimensionless space and time variables. Looking at the equation, water fractional flow is subsequently equal to mean water velocity, decided by the sum of the mean velocity of all flowing phases.

The concentration and fractional flux equations are as follows

$$C_i = C_{i1}f_1 + C_{i2}S_2 \tag{17}$$

$$F_i = C_{i1}f_1 + C_{i2}f_2 \tag{18}$$

The components of oil, water or miscible solvent are distributed between aqueous (1) and oleic (2) phases. By taking the effects of viscous fingering, flux in Eq.17 is modified to

$$F_i = C_{i1}f_1 + f_{i2}f_2, \quad i = 1,2,3 \tag{19}$$

where

$$f_{i2} = \frac{C_{i2}/\mu_i}{(C_{12}\mu_1 + C_{22}\mu_2 + C_{32}\mu_3)} \tag{20}$$

Using the equation of Koval factor

$$K = H[0.78 - 0.22(\frac{\mu 2}{\mu 3})^{1/4}]^4 \quad (21)$$

It is substituted into Eq.19 to form the following equations

$$f_{32} = \frac{C_{32}}{\left(C_{12}\left(\frac{\mu_3}{\mu_1}\right)+\frac{C_{22}}{K}+C_{32}\right)} \quad (23)$$

$$f_{22} = \frac{\frac{C_{22}}{K}}{\left(C_{12}(\frac{\mu_3}{\mu_1})+\frac{C_{22}}{K}+C_{32}\right)} \quad (24)$$

$$f_{12} = 1 - f_{22} - f_{32}$$

2.5.2 Vertical Heterogeneity

Heterogeneity plays an important role in flooding operations. One aspect of heterogeneity is permeability variation. Sweep efficiency also largely depends on areal heterogeneity in different intervals and its effects have largely been approximated by "fudge factors" (Singhal & Springer, 2006). Vertical heterogeneity can be defined by a ratio of net to gross pay thickness, ratio of vertical to horizontal permeability, or a variation of measured core permeability. Core permeability is a part of the Dykstra-Parsons equation's *V*- factor.

In oil reservoirs where the vertical to horizontal permeability ratio is low, the importance of oil recovery by CO_2 flooding is even higher. Reservoir heterogeneity of large changes in permeability is one of the most important factors towards the success of CO_2 flooding (Shedid, 2009). Vertical reservoir heterogeneities are at times severely hindered due to the pay being interspersed with intervals of impervious shale and anhydrite.

2.5.3 Gravity Segregation

A major problem with gas EOR especially in heterogeneous formations would be vertical segregation of gas under gravity (Rossen et al., 2010). Stone (1982) has come up with a useful model for gravity segregation which was further elucidated by Jenkins (1984). Both involve steady state, uniform coinjection of gas and water in a homogeneous porous medium.

Below would be derived equations from Stone and Jenkins where L_g being rectangular reservoirs and R_g representing cylindrical reservoirs:

$$L_g = \frac{Q}{k_z(\rho_w - \rho_g)gW\lambda_n^m} \tag{25}$$

$$R_g = \sqrt{\frac{Q}{\pi k_z(\rho_w - \rho_g)g\lambda_n^m}} \tag{26}$$

CHAPTER 3 METHODOLOGY

3.1 Screening Model Flow

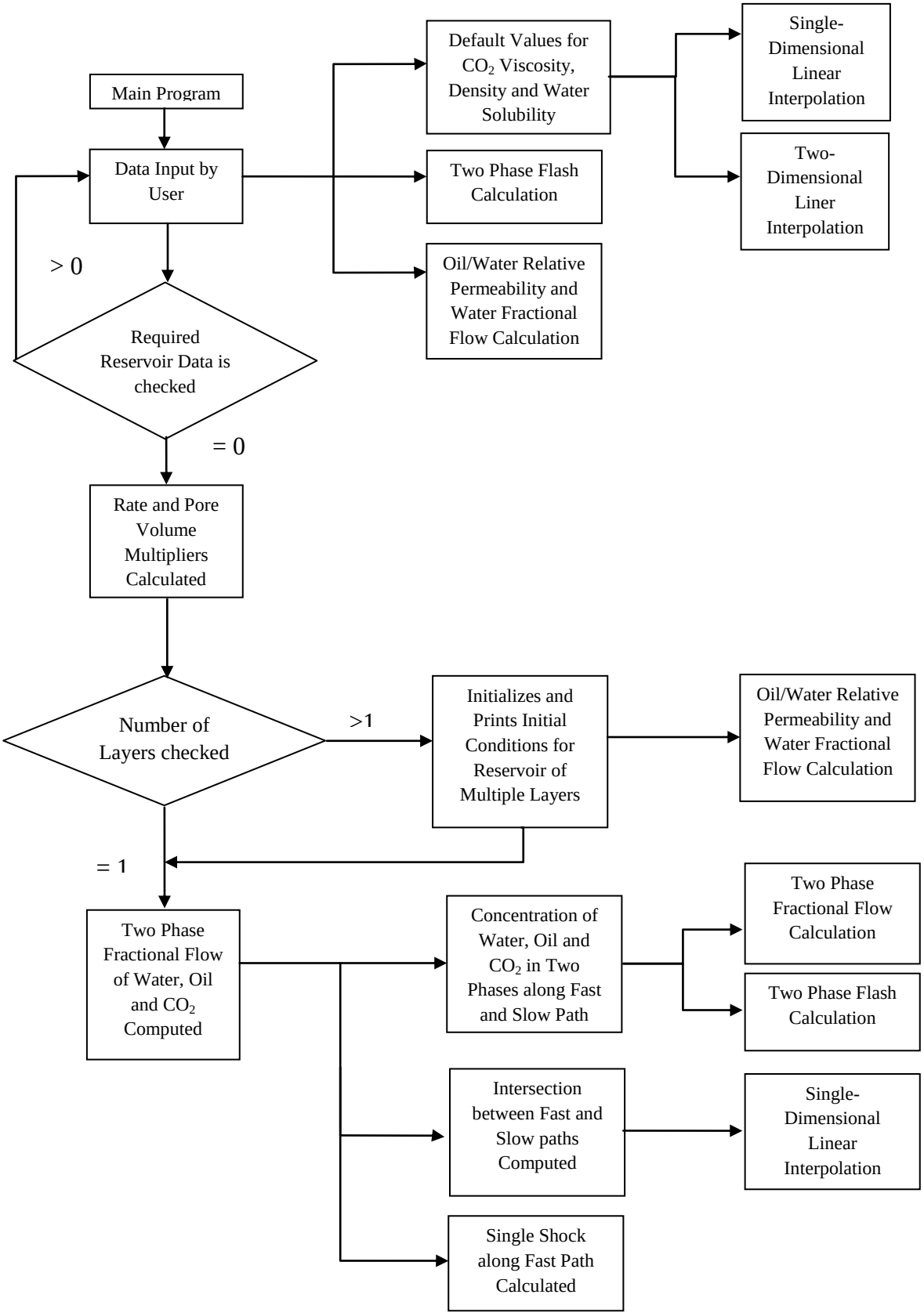

3.2 Project Methodology and Planner

In order to achieve the objectives of the project, several key factors have to be taken into account so that research and execution is done in a systematic manner. The methodology created, describes four main phases in the execution of the project.

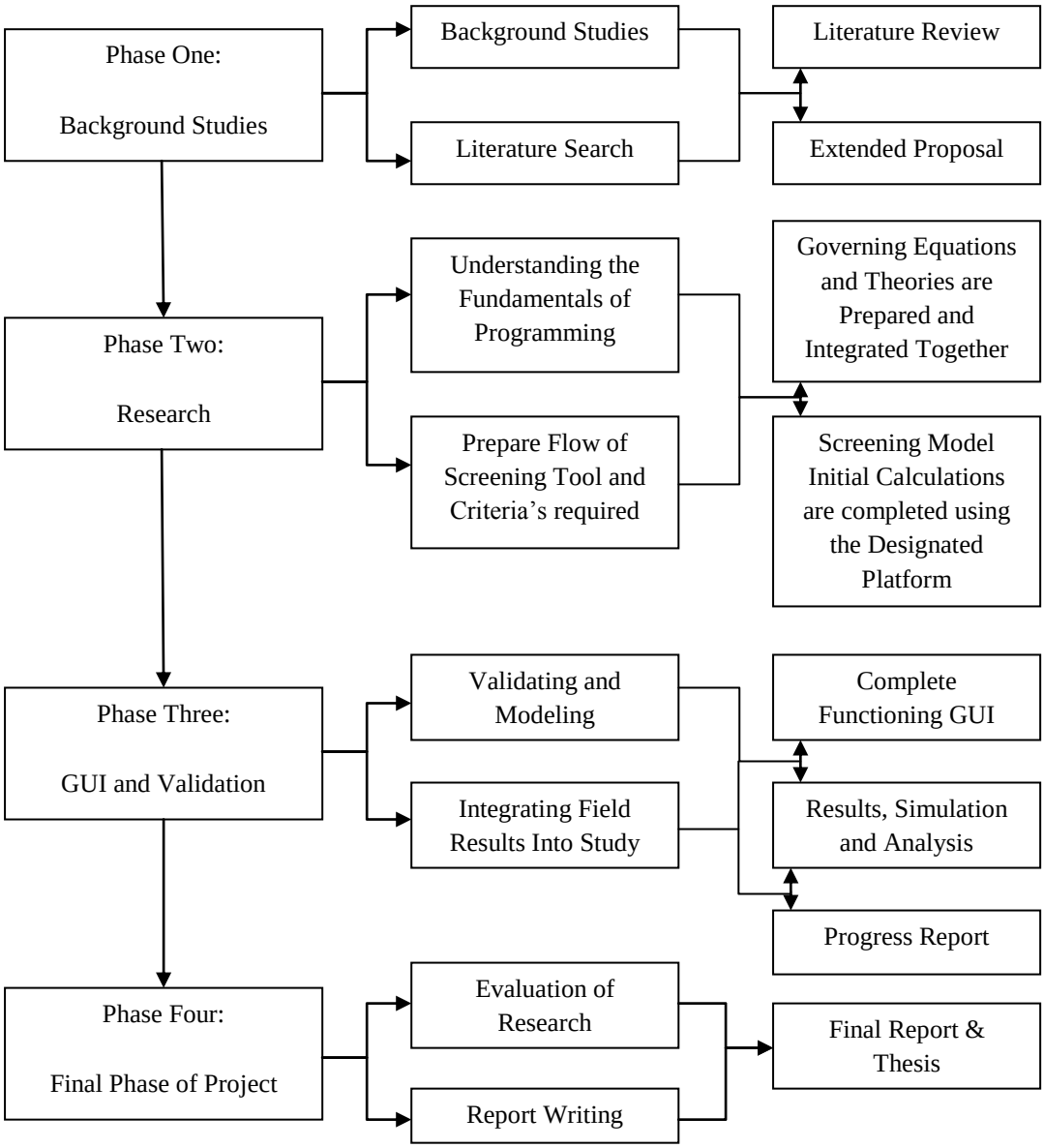

3.3 Gantt Chart

No	Description	1	2	3	4	5	6	7	8	9	10	11	12	13	14
1	Topic Selection	■													
2	Topic studies and familiarization –Background Study -Literature Review Reading		■	■	■	■									
3	Familiarizing with simulation program				■	■	■	■							
4	Extended Proposal Preparation and Submission						■	■							
5	Extended Proposal Defense Presentation								■						
6	Continuation of Project								■	■	■	■	■		
7	Interim Report											■		■	
No	**Description**	**1**	**2**	**3**	**4**	**5**	**6**	**7**	**8**	**9**	**10**	**11**	**12**	**13**	**14**
1	Continuation of Research Work	■	■	■	■	■	■	■							
2	Submission of Progress Report								■						
3	Research Work Continues								■	■	■	■	■		
4	Completion of Screening Tool										■	■	■		
5	Result Evaluation and Discussion										■	■	■		
6	Final report											■	■		
7	Pre-SEDEX											■	■		
8	Submission of Reports											■	■		
9	Oral Presentation											■	■		

1) ☼ - Represents Personal Milestones

3.4 Future Milestones

- Next step would be to test the screening model with field data if the required parameters and outputs are produced.
- Improve on the GUI of the screening tool so that it is user friendly and has ease of operation
- Completing the thesis of the research project

CHAPTER 4 VALIDATIONS, RESULTS AND DISCUSSIONS

3.1 Initial Computation

The screening model initially starts with a series of inputs by the user which includes the case controls that specifies the reservoir calculation methods where when this input is equivalent to 1, 1-Dimensional reservoir calculations are computed which includes the Koval factor. In terms of the output printing, a value of 1, directs the program to print out the initial properties of the CO_2 fluid flow and a value of 3, prints out the 1-Dimensional summary for production and injection. Next would be the indicator for solubility where a value of 0, specifies that CO_2 solubility in water is not accounted for, and water alternating gas calculations are not done, whereas a value of 1, allows the solubility of CO_2 in water to be calculated from PVT tables specified in the screening tool.

Once the viscosities, density and solubility of CO_2, oil and water have been computed, the oil and water relative permeability, water fractional flow and derivates are computed. These values are computed using Corey-type equations. Listed below would be the equations that are used in the screening tool

$$k_{rw} = k_w \times {U_w}^{E_w} \tag{27}$$

where

$$U_w = \frac{\left(S_{wf2} - S_{wf1}\right)}{1.0 - S_{wf1} - S_{ow}} \tag{28}$$

and

$$k_o = k_o \times {U_o}^{E_o} \tag{29}$$

where

$$U_o = \frac{1.0 - S_{wf2} - S_{ow}}{1.0 - S_{wf1} - S_{ow}} \tag{30}$$

The equation above basically shows the relative permeability of water, k, and the relative permeability of oil, k_{ro}, where E_w is the exponent for water relative permeability and $E_o$for oil, S_{wf2} is for the connate water saturation and S_{wf1}would be the initial water saturation while $S_{ow}$is the residual oil saturation to water. k_w and k_o are the relative permeability of connate water and oil at residual saturation.

Next the water fractional flow is calculated using the following equations

$$f_w = \frac{1.0}{1.0 + W_{mob}} \tag{31}$$

Where

$$W_{mob} = \frac{k_o \times \mu_w}{\mu_o \times k_w} \tag{32}$$

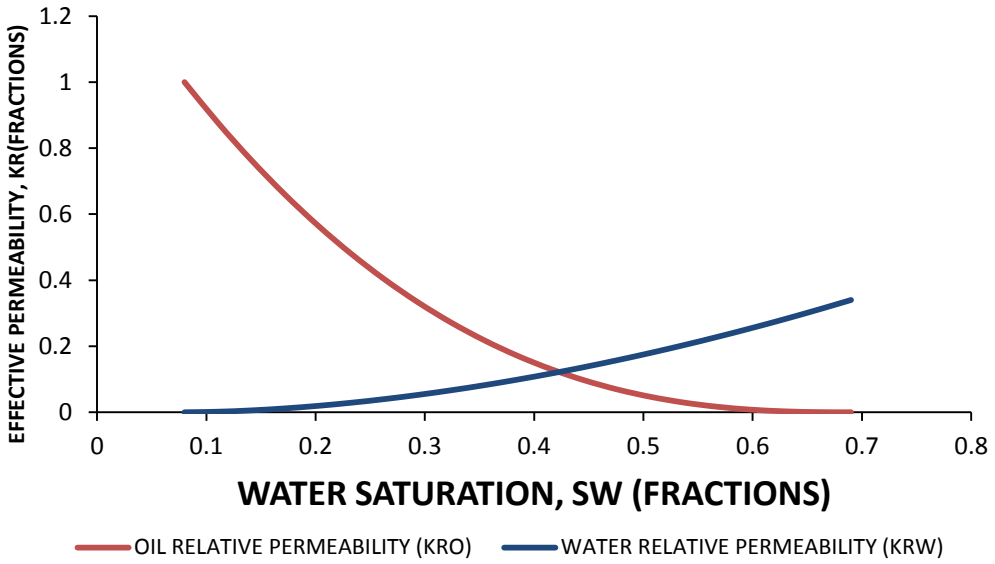

Figure 4.1-- Relative Permeability Chart

Fig.4.1, shows the relative permeability curves for oil and water versus water saturation. Hence, from the curves it can be deduced that as the saturation of water increases the effective permeability increases and thus causing the effective permeability of oil to increase gradually. Since the process is a water alternating gas (WAG) process the fraction of water to oil is processed at the same time using the screening tool.

3.2 Fractional Flow Calculations

The most important theory that's included into the screening tool would be the fractional flow theory. One dimensional fractional flow equation by method of characteristics is introduced into the calculations and results into two characteristic velocities; fast path that passes through initial reservoir conditions and the slow path that goes through the injected conditions. The effects of viscous fingering were included into the screening tool by modifying the fractional flow using the Koval Factor. The value of the Koval factor does not change when the screening tool is run.

The heterogeneity factor is calculated in two ways depending on the value of Dykstra-Parsons coefficient (V_{DP}). Whereby:

When V_{DP} is greater than 0

$$H = 10.0^{\left(V_{DP}\right)/(1.0-V_{DP})^{0.2}} \tag{33}$$

or, if V_{DP} is less than 0 and the V_{DPL} (Dykstra-Parsons coefficient for reservoir heterogeneity among all layers) is greater than 0

$$H = 10.0^{\left(V_{DPL}(i)\right)/(1.0-V_{DPL}(i))^{0.2}} \tag{34}$$

In the case of the calculations being done with only one layer a constant value of $V_{DP}$is used throughout the screening tool's run, however if the layer are of two and above, the V_{DPL} would influence the heterogeneity of the reservoir thus causing the Koval factor to be different across the varying layers where i = 2,3,4,5.

Once the initial conditions and reservoir properties have been calculated, the effects of gravity segregation are taken into play, before fractional flow paths are calculated.

3.2.1 Effects of Gravity Segregation

Taking into consideration the density of CO_2 compared to oil or water (CO_2 is less dense than oil and water), it has to be modeled accordingly in the screening tool. The method used would be to increase the Koval factor for each layer by multiplying it with a factor. In a reservoir, the CO_2 would move towards the top and will eventually override oil in lower zones.

A gravity override factor, F_{act}, is used in this case, where:

$$F_{act} = 0.565 \times Arc \log D_G + 0.870 \tag{35}$$

the equation for dimensionless gravity number D_G would be as follows:

$$D_G = 2.571 \times \ k_{RVH} \times A \times k_R \times \frac{\rho_w - \rho_g}{q_t \times \ \mu_g} \tag{36}$$

where K_{RVH} is the ratio of vertical to horizontal permeability, and ρ_w and ρ_g are the density of water and CO_2 respectively, A stands for the area, K_R is the reservoir permeability, and q_{rt} would be the total injection rate. As the gravity override factor increases, the Koval factor increases and thus causes recovery to decrease. The dimensionless gravity numberD_G, is the ratio of time required for a liquid particle to travel the distance between wells to the time required for the fluid to move from the bottom of the reservoir to the top.

Hence, once the computation of $D_G$is done in the screening tool, the gravity override factor F_{act} is further calculated. This factor influences the Koval factor that would be used in the calculation of fractional flow. A value of $F_{act} = 1$, will prompt the program to not used the effects of gravity segregation.

Once these values have been computed and identified two phase flash and fractional flow calculations are done. PVT calculations are used in two phase flash where they are to obtain vapor/liquid equilibrium data. Oil and CO_2 flux, and their concentration are calculated and plotted from the fractional flow calculations.

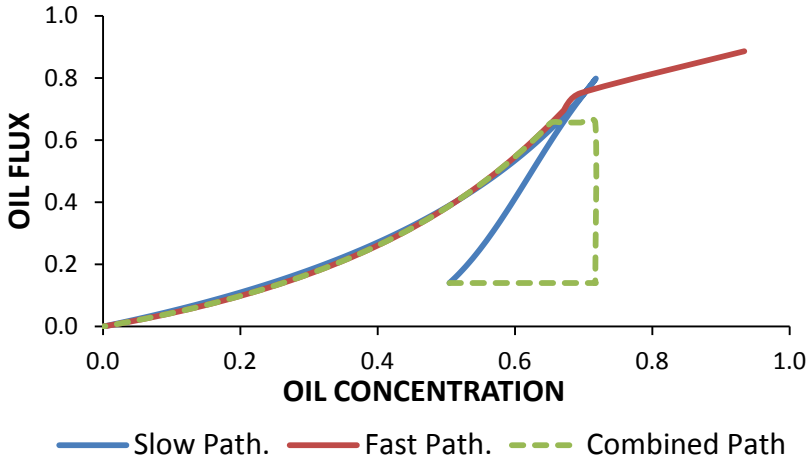

Figure 4.2 – Oil Flux versus Concentration Plot

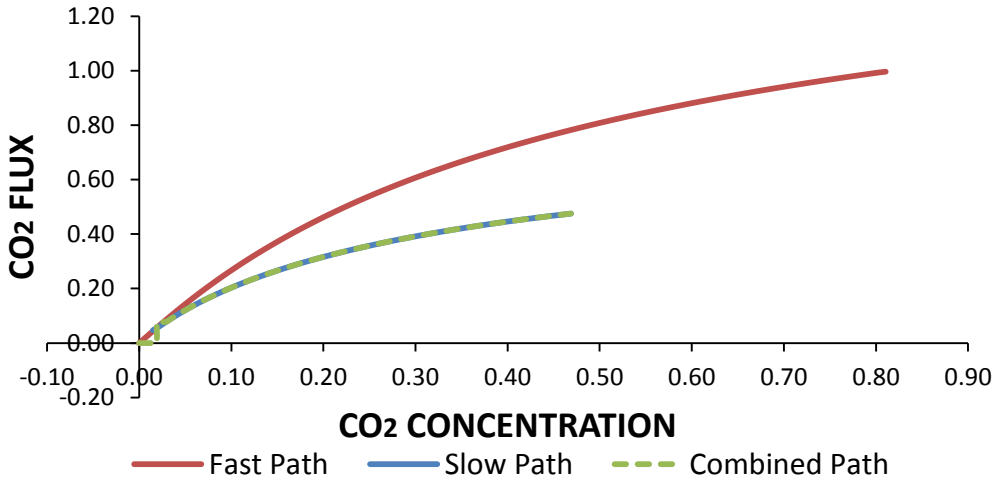

Figure 4.3 – CO2 Flux versus CO2 Concentration Plot

The figures 4.2 and 4.3 fast, slow and combined paths for fractional flow. Equations 5 to 13 explain on how these curves are plotted. The intersection between the paths are show in figure 4.2, this is where the paths switch from the fast path to the slow path. Shocks are introduced into the fast path curve so that the curvature is monotonous. The combined path is where the fast and slow path array results are joined together.

3.3 Rate and Slug Size Multipliers for Layers

From the fractional flow theory, it can be seen that V_{DPL} is used to allocate the total injection rate,q_{rt} and at the same time the V_{PV}, which represents the total hydrocarbon pore volumes of CO_2 and water that is injected during WAG.

The cumulative probability of permeability of a layer, k_i, with *n* layers is shown below:

$$k_i = \quad (1\text{-}0.5)/\mathrm{n} \tag{37}$$

The rate and slug size is then approximated by the number of layers by:

$$V_{PV(i)} = n(q_{rt(i)} / q_{rt})\ V_{PV} \tag{38}$$

Several outputs are retrieved from the slug rate and size calculations which would be the average oil concentration, average CO_2 concentration, incremental production for oil and CO_2 and the value of dimensionless time to ultimate concentration. The fractional fluxes are converted into a 1-Dimensional injection/production summary.

3.4 1-Dimensional Production Summary

Once the fractional flow, shock and also finite slug calculation have taken place then the screening tool computes all this data together to finally come up with a production summary of the particular reservoir which data has been inputted by the user.

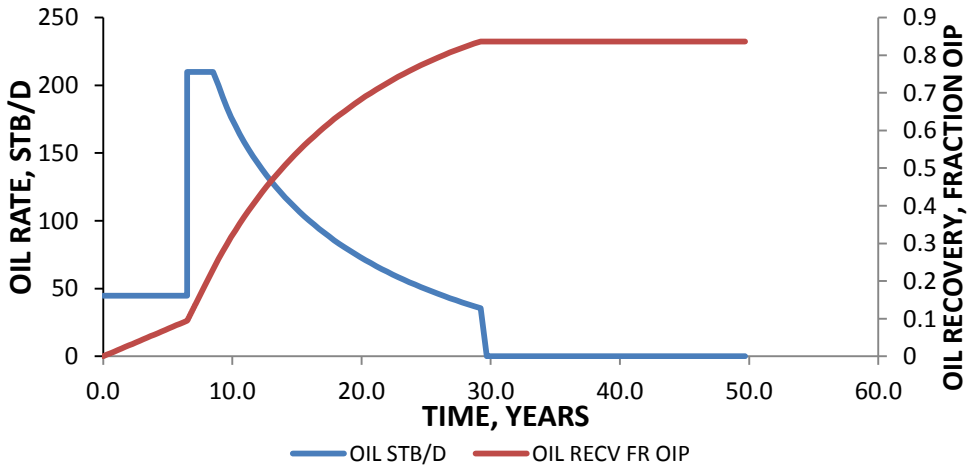

Figure 4.4—Oil Production Recovery Rate Plot

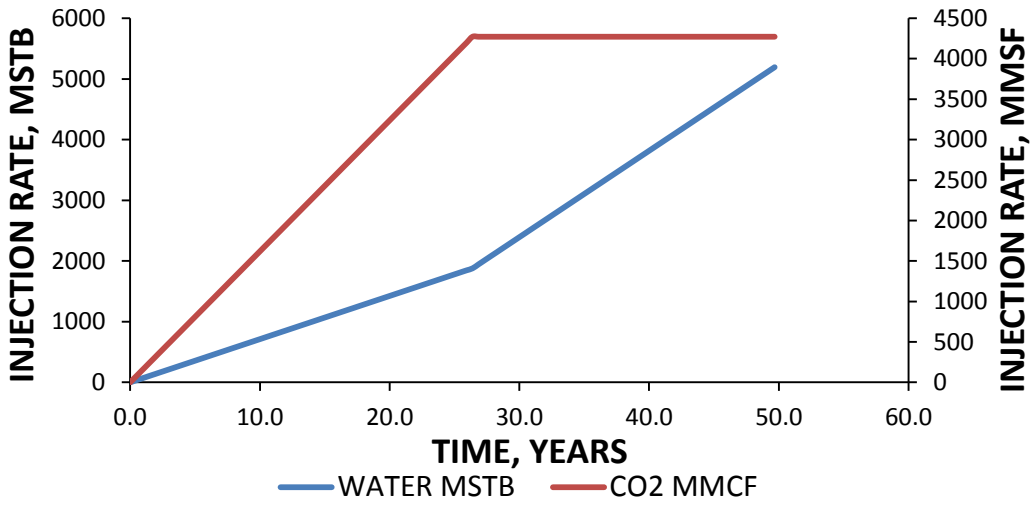

Figure 4.5 – Cumulative Injection Rates Plot

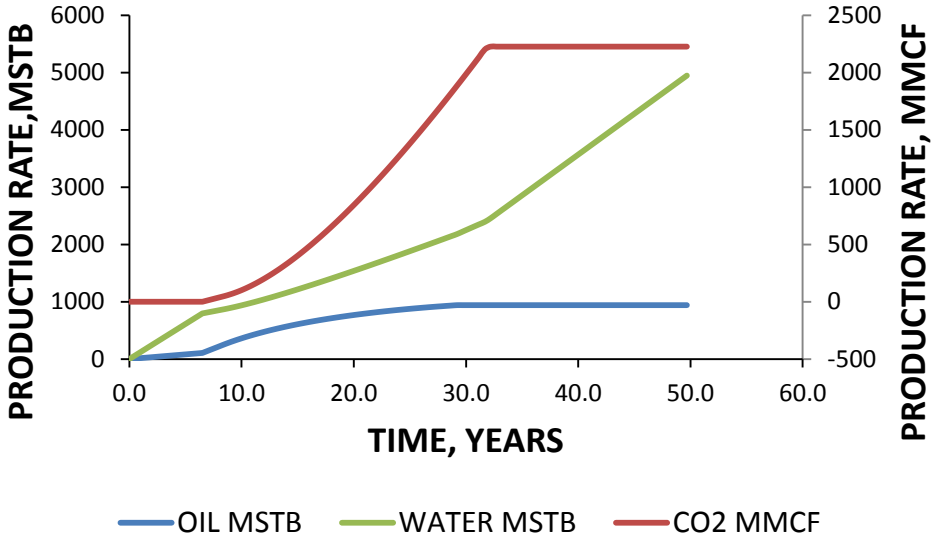

Figure 4.6 – Cumulative Production Rates Plot

From Figure 4.4 it can be seen that the oil rate has an increase at around 6 years of CO_2 injection and after a peak in production, the production starts to decrease. The cumulative production of oil can be seen from Figure 4.6 where maximum oil retrieved from the reservoir would be at around 28 years and after that the CO_2 flooding will no longer be economical as the well has depleted in oil reserves.

3.5 Data Validation

Figures 4.1 – 4.6 are derived from the screening of raw data using CO_2 MIST. These graphs can be validated using values obtained from Paul et al.,(1984) where the paper provides initial reservoir and injection conditions that can be incorporated into CO_2 MIST.

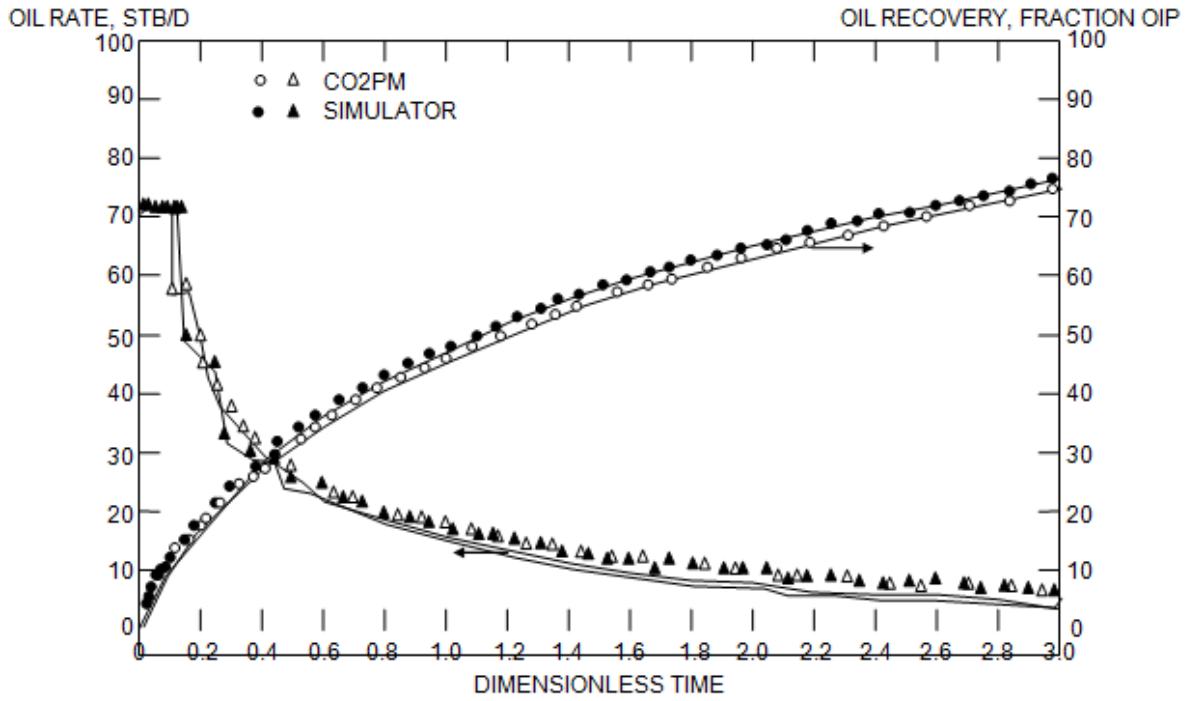

Figure 4.7 – 1-D Secondary Case Data. Paul et.al (1984)

Figure 4.7 shows the 1-D secondary case data plot from Paul et al., (1984). The paper compares this data to a CO_2 miscible flooding simulator and by comparison to Figure 4.4 which is from CO_2 MIST, the plot obtained shows almost similar comparison in terms of oil recovery and the oil rate. To add-on, CO_2 MIST is believed to show more in depth curvature and data points compared to the study done by Paul et al., (1984). The time in CO_2 MIST is however in terms of years and the plot in the validation study describes the 1-D case study in dimensionless time.

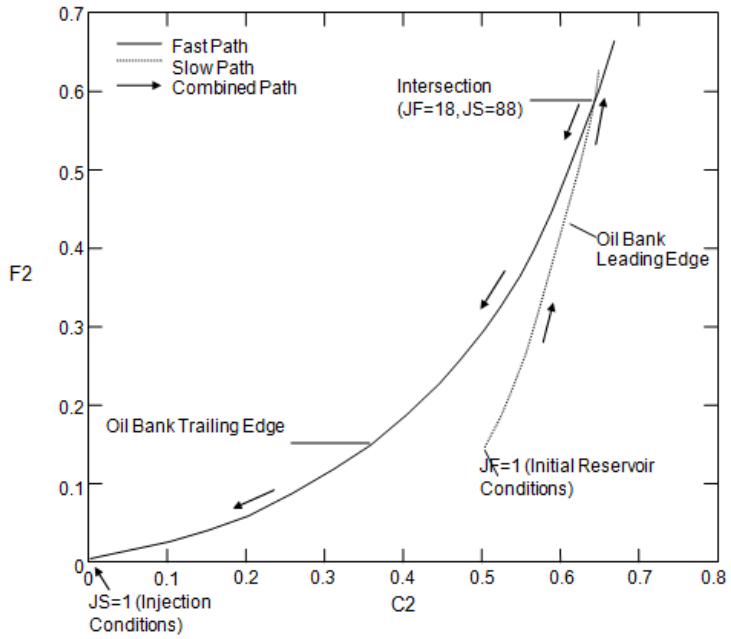

Figure 4.8 – Oil Flux versus Concentration Plot. Paul et.al (1984)

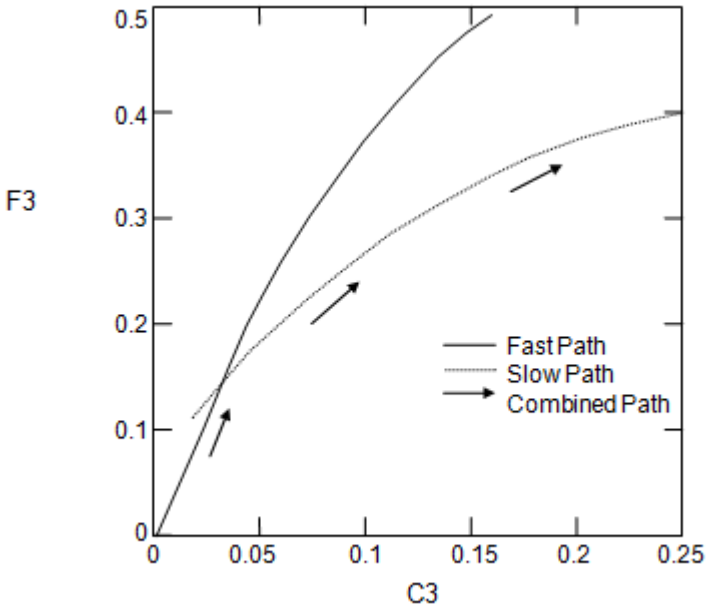

Figure 4.9 – CO_2 Flux versus Concentration Plot. Paul et.al (1984)

Figures 4.8 and 4.9 describe the oil flux and carbon dioxide flux versus concentration plot by the paper published by Paul et al., (1984) and these plots when compared to Figures 4.2 and 4.3 which is obtained using CO_2 MIST by incorporating raw data from the research done by Paul et. al, (1984) shows similar characteristics. It can be seen that the intersection of the fast path and slow paths in fractional flow happen at the same points and the data points are of similar nature. However, through observation it can be said that CO_2 MIST provides better precision in terms of its data presentation where more data points are available and at the same time the combined path of both the fast path and slow path is shown in-depth.

Chapter 5 CO_2 MIST User Guide

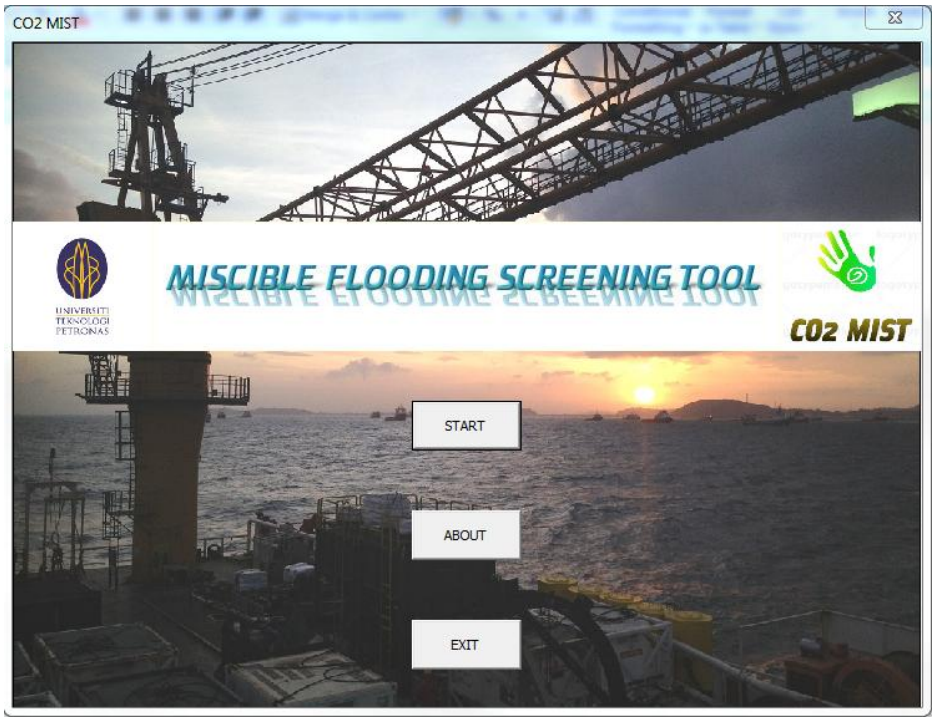

Figure 5.1-- CO_2 MIST Loading Page

Figure 5.1 shows the start page of the screening tool where the START button directs the user to the user input page, the ABOUT button directs the user to a page where a brief introduction of the screening tool is available and lastly the EXIT button exits the program.

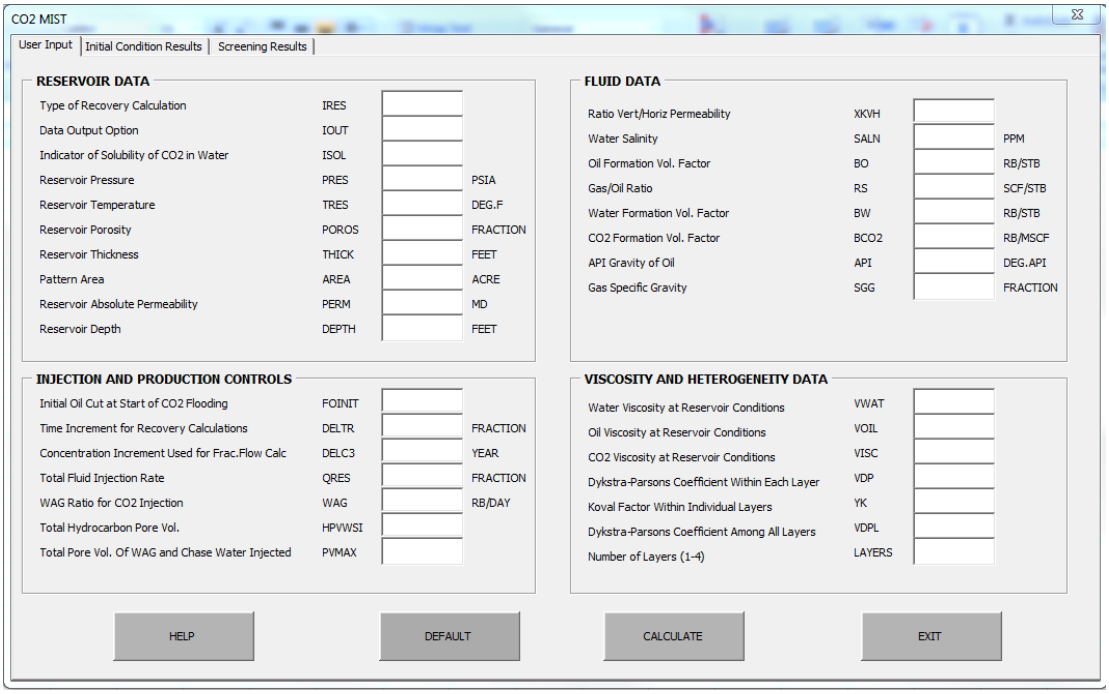

Figure 5.2 – User Input Page

Figure 5.2 shows the user input page for the screening tool where the user needs in to key in the reservoir data, injection and production controls, fluid data and lastly the viscosity and heterogeneity data. The reservoir data inputs include the pressure, temperature, thickness, area, permeability and the depth of the reservoir. The injection and production controls, and fluid data includes information about the fluid injected which would be CO_2 and water. The HELP button at the bottom of the input page provides the user information on the type of recovery calculations and data output options available in the program, and most importantly points out what each input represents. The DEFAULT button when clicked automatically inputs default values and thus calculations is done using the default values inputted. Lastly, when all data has been filled in the CALCULATE button is required to be clicked and thus the screening evaluation is done.

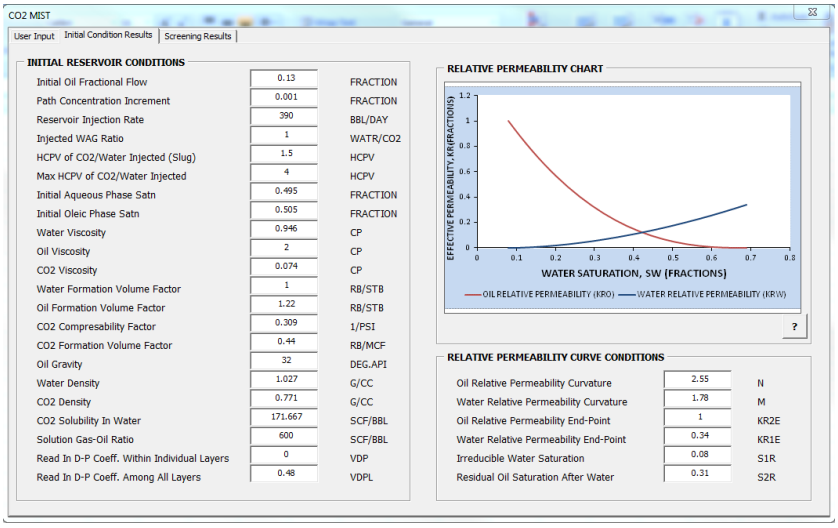

Figure 5.3 – Initial Condition Results

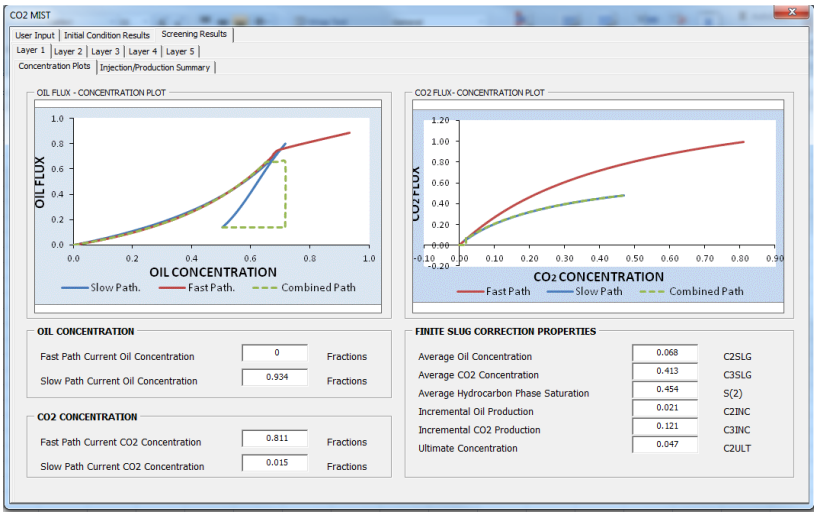

Figure 5.4 – Concentration Plots

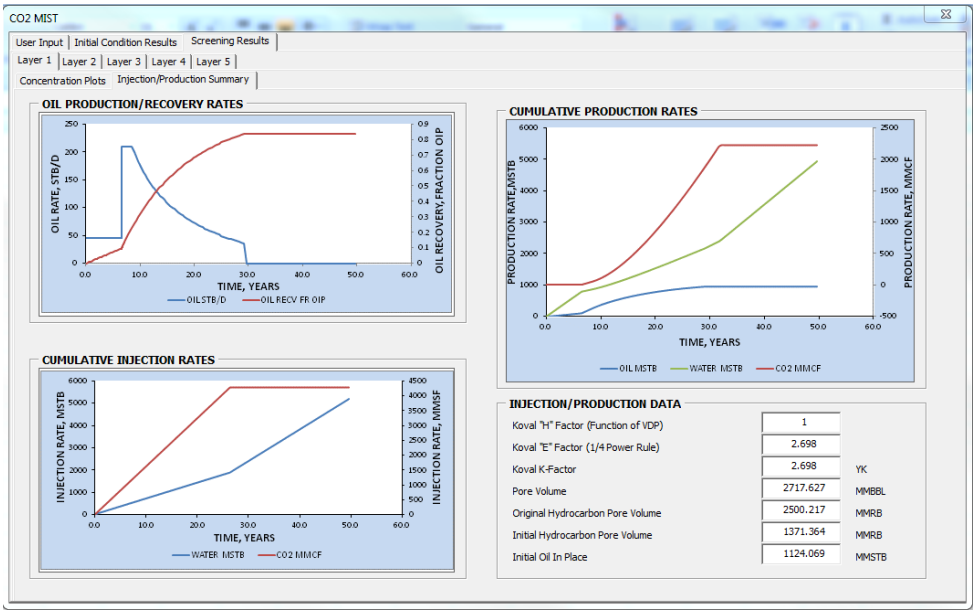

Figure 5.5 – Injection and Production Summary

Figures 5.3 – 5.4 show the screening results of the default values that had been inputted in the user input page. Figure 5.3 shows the initial reservoir conditions and the relative permeability curve conditions. The initial conditions results are further plotted into a relative permeability chart that shows oil and water relative permeability curves. Next the screening results would be divided into a concentration plot tab and an injection/ production summary. The concentration plot tab shows fractional flow results and finite slog correction properties. Fast and slow path fractional flow plot are displayed on this tab. Lastly, the screening tool displays the production and recovery rate plots that conclude the evaluation of the reservoir for CO_2 miscible injection

CHAPTER 6 CONCLUSION

6.1 Conclusion

It can be concluded that the screening model for CO_2 miscible flooding is certainly a method that can be used into the further study and also the wide implementation of CO_2 flooding in especially areas that have not ventured into its usage. Due to the wide environmental values, the model would certainly play apart in reservoir functions and operations. The model applies numerical simulations and research data that have been proven by various other publications and field laboratory experiments.

Nomenclature

S_w = *Saturation of water*

S_g = *Saturation of CO_2*

f_w = *Fractional flow of water*

f_g = *Fractional Flow of CO_2*

f_o = *Fractional Flow of Oil*

k_{rw} = *Relative Permeability of Water*

k_{rg} = *Relative Permeability of CO_2*

k_{ro} = *Relative Permeability of Oil*

μ_g = *Viscosity of CO_2*

μ_w = *Viscosity of Water*

μ_o = *Viscosity of Oil*

σ = *Characteristic Velocity*

C = Concentration

F = Flux

K = Koval Factor

H = Heterogeneity Factor

k_z = *Vertical Permeability Gravitational Acceleration*

W = Thickness of the Rectangular Reservoir Perpendicular to Flow

E_w = *Exponent for Water Relative Permeability*

E_o = *Exponent for Oil Relative Permeability*

S_{wf2} = *Connate Water Saturation*

S_{wf1} = *Initial Water Saturation*

S_{ow} = *Residual Oil Saturation*

K_w = *Relative Permeability of Connate Water at Residual Saturation*

K_o = *Relative Permeability of Oil at Residual Saturation*

V_{DP} = *Dykstra-Parsons Coefficient*

V_{DPL} = *Dykstra-Parsons Coefficient for Reservoir Heterogeneity among all Layers*

F_{act} = *Gravity Override Factor*

D_G = *Dimensionless Gravity Number*

K_{RVH} = *Ratio of Vertical to Horizontal Permeability*

ρ_w = *Density of Water*

ρ_g = *Density of* CO_2

k_R = *Reservoir Permeability*

q_{rt} = *Total Injection Rate*

n = *No. of Layers*

k_i = *Cumulative Probability of Permeability of a Layer*

V_{PV} = *Total Hydrocarbon Pore Volume*

REFERENCES

1. Andrei, M., Simoni, M. D., Delbianco, A., Cazzani, P., & Zanibella, L. (2011). Enhanced Oil Recovery with CO_2 Capture and Sequestration.

2. Asghari, K., & Dong, M. (2007). Development of a Correlation Between Performance of CO_2 Flooding and the Past Performance of Waterflooding in Weyburn Oil Field, Vol. 22 pg 260-264, SPE 99789 -PA.

3. Brinkman, F. K., & Miertschin, J. E. (1998). Use of Full-Field Simulation to Design a Miscible CO_2 Flood, SPE/DOE Improved Oil Recovery Symposium, 19- 22 April 1998, SPE 39629.

4. Chen, S.M., & Olynyk, J. (1985). Sweep Efficiency Improvement Using Horizontal Wells or Tilted Horizontal Wells in Miscible Floods, Annual Technical Meeting of The Petroleum Society of CIM, 2-5 June 1985.

5. F.M. Orr Jr., R. J. (1993). Development of Miscibility in Four-Component CO2 Floods. *SPE Reservoir Engineering*, 135-142.

6. Henry, R., & Metcalfe, R. (1983). Multiple-Phase Generation During carbon Dioxide Flooding. *SPE Journal* , 595-601.

7. Ikhsan, A., Sugiatmo, & Idris, A. K. (1998). The CO_2 Flooding: Prospect and Challenges on Malaysian Oil Fields.

8. Islam, M.R., & Saghir, Z. (1999). Experimental and Numerical Modeling Studies of Viscous Fingering, CSPG and Petroleum Society Joint Convection, Annual Technical Meeting, 14-18 June 1999.

9. Juanes, R. (2006). Impact of Viscous Fingering on the Prediction of Optimum WAG Ratio, 2006 SPE/DOE Symposium on Improved Oil Recovery, 22-26 April 2006, SPE 99721.

10. Kleppe, J. (2011). Buckley-Leverett Analysis.

11. McCoy, S. T., & Rubin, E. S. (2006). A Model of CO_2-Flood Enhanced Oil Recovery with Applications to Oil Price Influence on CO_2 Storage Costs.

12. Melzer, S. L. (2012). Carbon Dioxide Enhanced Oil Recovery (CO_2 EOR): Factors Involved in Adding Carbon Capture, Utilization and Storage (CCS) to Enhanced Oil Recovery.

13. Orr, F., Heller, J., & Taber, J. (1982). Carbon Dioxide Flooding for Enhanced Oil Recovery: Promise and Problems, Annual Meeting of the American Oil Chemists Society, 2-6 May 1982, SPE 22637 - PA.

14. Paul, G.W., Lake, L. W., & Gould, T. L., (1984). A Simplified Predictive Model for CO_2 Miscible Flooding, 59th Annual Technical Conference and Exhibition, 16-19 September 1984, SPE 13238.

15. Pontious, S. B., & Tham, M. J. (1978). North Cross (Devonian) Unit CO_2 Flood - Review of Flood Performance and Numerical Simulation Model, SPE 6390 - PA.

16. Pope, G. (1980). The Application of Fractional Flow Theory to Enhanced Oil Recovery. *SPE Journal* , 191-205.

17. Prieditis, J. B. (1993). Effects of Recent Relative Permeability Data on CO_2 Flood Modeling, 68th Annual Technical Conference and Exhibition of the Society of Petroleum Engineers, 3-6 October 1993, SPE 26650.

18. Rao, D. N., & Hughes, R. G. (2011). Current Research and Challenges Pertaining to CO_2 Flooding and Sequestration Vol 7 pg 17 -19.

19. Rossen, W.R., Duijn, C.J., Nguyen, Q.P., Shen, C., & Vikingstad, A.K. (2010). Injection Strategies To Overcome Gravity Segregation in Simultaneous Gas and Water Injection Into Homogeneous Reservoirs, Vol. 15 pg 76-90, SPE 99794.

20. S. Wo, S.A.,& and Mullen, E. P. (2008). Simulation Evaluation of Gravity Stable CO_2 Flooding in the Muddy Reservoir at Grieve Field, Wyoming, SPE/DOE Improved Oil Recovery Symposium, 19-23 April 2008, SPE 113482.

21. Saripalli, P., & McGrail, P. (2001). Semi-Analytical Approaches to Modelling Deep Well Injection of CO_2 for Geological Sequestration, Vol. 43 pg 185-198.

22. Shah, M. (2008). *Potential of CO_2 Flooding in Appalachian Basin.*

23. Shedid, S. (2009). Influences of Different Modes of Reservoir Heterogeneity on Performance and Oil Recovery of Carbon Dioxide Miscible Flooding. *Journal of Canadian Petroleum Technology* , 29-36.

24. Singhal, A.K., Springer, S.J. (2006). Characterization of Reservoir Heterogeneity Based on Performance of Infill Wells in Waterfloods, Vol.45 no. 7, SPE 060704.

25. Srivastava, R., & Huang, S. (1997). Technical Feasibility of CO2 Flooding In Weyburn Reservoir-A Laboratory Investigation. *Journal of Canadian Petroleum Technology* .

26. Stalkup, F. I. (1978). Carbon Dioxide Miscible Flooding: Past, Present, And Outlook for the Future, Vol. 8 no. 8, SPE 7042-PA.

27. Toelle, B., & Pekot, S. D. (2007). CO_2 EOR From a North Michigan Silurian Reef, SPE Eastern Regional Meeting, 17-19 October 2007, SPE 111223.

28. Vetter, O., Bent, M., & Kandarpa, V. (1987). Three-Phase PVT and CO2 Partitioning. *SPE California Regional Meeting.* Ventura, California: Society of Petroleum Engineers.

29. Wood, D.J., Lake, L. W.,& Johns, R.T.(2008). A Screening Model for CO_2 Flooding and Storage in Gulf Coast Reservoirs Based on Dimensionless Groups, Vol. 11 pg 513-520, SPE 100021-PA

30. Yellig, W. F., & Metcalfe, R. S. (1980). Determination and Prediction of CO_2 Minimum Miscibility Pressures, Vol. 32 no. 1, SPE 7477 - PA.

31. Yongmao, H., Zenggui, W., Binshan, W., & Yueming, C. (2004). Laboratory Investigation of CO2 Flooding. *Nigeria Annual International Conference and Exhibition.* Abuja, Nigeria.

APPENDIX

RESERVOIR AND INJECTION DATA			
CASE CONTROLS			SHORT
RESERVOIR CALC METHOD	3	IRES	IRES
OUTPUT CONTROL	10	IOUT	IOUT
ACCOUNT FOR CO2/WATER SOLUBILITY	1	ISOL	ISOL
NUMBER OF LAYERS	1	LAYERS	LAYERS
FORMATION PROPERTIES			SHORT
FORMATION PRESSURE	2000	PSIA	PRES
FORMATION TEMPERATURE	105	DEG.F	TRES
POROSITY	0.113	FRACTION	POROS
NET THICKNESS(PAY)	77.5	FEET	THICK
PATTERN AREA	40	ACRE	AREA
PERMEABILITY	6	MD	PERM
DEPTH	5000	FT	DEPTH
VERT/HORIZ PERMEABILITY RATIO	0.01	KV/KH	XKVH
RESERVOIR WATER SALINITY	50000	PPM	SALN
RELATIVE PERM CURVES			
OIL RELATIVE PERM CURVATURE	2.55	N	N
WATER RELATIVE PERM CURVATURE	1.78	M	M
OIL RELATIVE PERM END-POINT	1	KR2E	KR2E
WATER RELATIVE PERM END-POINT	0.34	KR1E	KR1E
IRREDUCIBLE WATER SATURATION	0.08	S1R	S1R
RESIDUAL OIL SATURATION AFTER	0.31	S2R	S2R
INITIAL CONDITIONS			
INITIAL OIL FRACTIONAL FLOW	0.13	FRACTN	FOINIT
PATH CONCENTRATION INCREMENT	0.001	FRACTN	DELC3
RESERVOIR INJECTION RATE	390	BBL/DAY	QRES
INJECTED WAG RATIO	1	WATR/CO2	WAG
HCPV OF CO2/WATER INJECTED (SLUG)	1.5	HCPV	HPVWS
MAX HCPV INJECTED (SLUG+ CHASE	4	HCPV	PVMAX
INITIAL AQUEOUS PHASE SATN	0.49538	FRACTN	SWI
INITIAL OLEIC PHASE SATN	0.50462	FRACTN	SOI
WATER VISCOSITY	0.9457	CP	V(1)
OIL VOSCOSITY	2	CP	V(2)
CO2 VISCOSITY	0.074	CP	V(3)
WATER FORMATION VOLUME FACTOR	1	RB/STB	BW
OIL FORMATION VOLUME FACTOR	1.22	RB/STB	BO
CO2 COMPRESSIBILITY FACTOR	0.3091	1/PSI	ZC
CO2 FORMATION VOLUME FACTOR	0.4397	RB/MCF	BCO2
OIL GRAVITY	32	DEG.API	API
WATER DENSITY	1.0265	G/CC	DENW
CO2 DENSITY	0.7709	G/CC	DC
CO2 SOLUBILITY IN WATER	171.667	SCF/BBL	SC
SOLUTION GAS-OIL RATIO	600	SCF/BBL	RS
COMBINED FAST/SLOW PATH			
PATH INTERSECT POINT	24	JF	JF
PATH INTERSECT POINT	92	JS	JS
CONCENTRATION AT INTERSECTION	0.71695	FAST	FAST
CONCENTRATION AT INTERSECTION	0.71695	SLOW	SLOW
CONCENTRATION AT INTERSECTION	0.01896	FRACTN	FRACTN

READ IN D-P COEFF WITHIN INDIV LAYERS	0	VDP
READ IN D-P COEFF AMONG ALL LAYERS	0.48	VDPL

RELATIVE PERMEABILITY TABLE				
WATER SATURATION (SW)	OIL EFFECTIVE PERM (KRO)	WATER EFFECTIVE PERM (KRW)	FRACTION WATER	DERIV DFW/DSW
0.0800	1.0000	0.0000	0.0000	0.0000
0.1105	0.8774	0.0016	0.0039	0.2466
0.1410	0.7644	0.0056	0.0154	0.5119
0.1715	0.6607	0.0116	0.0358	0.8421
0.2020	0.5661	0.0194	0.0675	1.2474
0.2325	0.4802	0.0288	0.1127	1.7240
0.2630	0.4027	0.0399	0.1732	2.2477
0.2935	0.3334	0.0525	0.2497	2.7671
0.3240	0.2718	0.0665	0.3411	3.2056
0.3545	0.2177	0.0821	0.4436	3.4764
0.3850	0.1708	0.0990	0.5508	3.5125
0.4155	0.1305	0.1173	0.6553	3.2970
0.4460	0.0967	0.1370	0.7498	2.8731
0.4765	0.0688	0.1579	0.8293	2.3267
0.5070	0.0464	0.1802	0.8914	1.7521
0.5375	0.0292	0.2037	0.9366	1.2236
0.5680	0.0165	0.2285	0.9670	0.7839
0.5985	0.0079	0.2546	0.9855	0.4475
0.6290	0.0028	0.2819	0.9953	0.2110
0.6595	0.0005	0.3103	0.9993	0.0635
0.6900	0.0000	0.3400	1.0000	0.0000

RESULTS SUMMARY LAYER 1 - FAST PATH

	C2-OIL	C3-CO2	C(2,2)	C(3,2)	S(OLEIC)	DIM VEL	DIM TIME	FOIL	FCO2
1	0.50453	0.00000	0.99010	0.00000	0.50462	2.00657	0.49836	0.14020	0.00000
2	0.51353	0.00000	0.99010	0.00000	0.51380	2.18264	0.45816	0.15905	0.00000
3	0.52353	0.00000	0.99010	0.00000	0.52400	2.37787	0.42054	0.18185	0.00000
4	0.53353	0.00000	0.99010	0.00000	0.53421	2.56951	0.38918	0.20660	0.00000
5	0.54353	0.00000	0.99009	0.00000	0.54441	2.75397	0.36311	0.23322	0.00000
6	0.55353	0.00000	0.99009	0.00000	0.55461	2.92754	0.34158	0.26164	0.00000
7	0.56353	0.00000	0.99009	0.00000	0.56481	3.08646	0.32400	0.29172	0.00000
8	0.57353	0.00000	0.99009	0.00000	0.57501	3.22709	0.30988	0.32331	0.00000
9	0.58353	0.00000	0.99009	0.00000	0.58522	3.34612	0.29885	0.35619	0.00000
10	0.59353	0.00000	0.99009	0.00000	0.59542	3.44065	0.29064	0.39015	0.00000
11	0.60353	0.00000	0.99009	0.00000	0.60562	3.50841	0.28503	0.42492	0.00000
12	0.61353	0.00000	0.99009	0.00000	0.61582	3.54784	0.28186	0.46022	0.00000
13	0.62353	0.00000	0.99009	0.00001	0.62602	3.55817	0.28104	0.49578	0.00000
14	0.63353	0.00000	0.99009	0.00001	0.63623	3.53949	0.28253	0.53129	0.00001
15	0.64353	0.00000	0.99009	0.00001	0.64643	3.49267	0.28631	0.56647	0.00001
16	0.65353	0.00000	0.99009	0.00001	0.65663	3.41935	0.29245	0.60105	0.00001
17	0.66353	0.00000	0.99009	0.00001	0.66683	3.32180	0.30104	0.63478	0.00001
18	0.67353	0.00000	0.99009	0.00001	0.67704	3.20282	0.31223	0.66742	0.00001
19	0.68353	0.00000	0.99009	0.00001	0.68724	3.06557	0.32620	0.69877	0.00001
20	0.69353	0.00001	0.99009	0.00001	0.69744	2.91360	0.34322	0.72868	0.00002
21	0.70353	0.00019	0.98983	0.00027	0.70783	2.86234	0.34936	0.75720	0.00055
22	0.71353	0.00364	0.98518	0.00492	0.72147	2.94836	0.33917	0.78599	0.01063
23	0.71786	0.01352	0.97216	0.01795	0.73577	2.94987	0.33900	0.79842	0.03988
24	0.71620	0.02352	0.95922	0.03090	0.74409	2.89276	0.34569	0.79344	0.06912
25	0.71235	0.03352	0.94642	0.04371	0.75019	2.81788	0.35488	0.78239	0.09769
26	0.70729	0.04352	0.93372	0.05641	0.75505	2.73604	0.36549	0.76828	0.12547
27	0.70143	0.05352	0.92110	0.06904	0.75910	2.65191	0.37709	0.75245	0.15241
28	0.69499	0.06352	0.90855	0.08159	0.76257	2.56784	0.38943	0.73561	0.17851
29	0.68811	0.07352	0.89606	0.09410	0.76559	2.48515	0.40239	0.71822	0.20377
30	0.68089	0.08352	0.88361	0.10655	0.76827	2.40459	0.41587	0.70055	0.22822
31	0.67339	0.09352	0.87119	0.11897	0.77066	2.32657	0.42982	0.68279	0.25188
32	0.66566	0.10352	0.85882	0.13136	0.77282	2.25132	0.44418	0.66508	0.27476
33	0.65773	0.11352	0.84647	0.14371	0.77478	2.17894	0.45894	0.64751	0.29691
34	0.64963	0.12352	0.83414	0.15604	0.77657	2.10943	0.47406	0.63014	0.31835
35	0.64139	0.13352	0.82185	0.16835	0.77821	2.04276	0.48953	0.61302	0.33911
36	0.63302	0.14352	0.80957	0.18064	0.77973	1.97888	0.50534	0.59619	0.35921
37	0.62454	0.15352	0.79730	0.19291	0.78113	1.91768	0.52146	0.57966	0.37870
38	0.61596	0.16352	0.78506	0.20516	0.78243	1.85908	0.53790	0.56346	0.39758
39	0.60729	0.17352	0.77283	0.21740	0.78364	1.80296	0.55464	0.54758	0.41588
40	0.59854	0.18352	0.76061	0.22962	0.78477	1.74922	0.57168	0.53204	0.43364
41	0.58972	0.19352	0.74840	0.24183	0.78583	1.69774	0.58902	0.51683	0.45088
42	0.58083	0.20352	0.73621	0.25404	0.78682	1.64843	0.60664	0.50196	0.46760

RESULTS SUMMARY LAYER 1 - SLOW PATH

	S.C2-OIL	S.C3-CO2	C(2,2)	C(3,2)	S(OLEIC)	DIM VEL	DIM TIME	S.FOIL	S.FCO2
1	0.00000	0.46886	0.00000	0.99066	0.43530	0.38427	2.60237	0.00000	0.47528
2	0.00514	0.46436	0.01162	0.97904	0.43640	0.38900	2.57069	0.00199	0.47354
3	0.01086	0.45936	0.02451	0.96614	0.43764	0.39435	2.53583	0.00423	0.47158
4	0.01661	0.45436	0.03737	0.95328	0.43890	0.39979	2.50132	0.00651	0.46959
5	0.02237	0.44936	0.05019	0.94044	0.44017	0.40532	2.46716	0.00883	0.46757
6	0.02816	0.44436	0.06299	0.92764	0.44146	0.41096	2.43334	0.01119	0.46552
7	0.03397	0.43936	0.07576	0.91487	0.44277	0.41669	2.39985	0.01359	0.46345
8	0.03979	0.43436	0.08849	0.90212	0.44411	0.42253	2.36670	0.01604	0.46135
9	0.04564	0.42936	0.10120	0.88941	0.44546	0.42847	2.33388	0.01853	0.45922
10	0.05151	0.42436	0.11387	0.87673	0.44683	0.43452	2.30138	0.02106	0.45705
11	0.05740	0.41936	0.12651	0.86408	0.44822	0.44068	2.26920	0.02364	0.45486
12	0.06332	0.41436	0.13912	0.85147	0.44963	0.44696	2.23733	0.02626	0.45264
13	0.06925	0.40936	0.15169	0.83889	0.45106	0.45336	2.20577	0.02893	0.45038
14	0.07521	0.40436	0.16422	0.82635	0.45252	0.45987	2.17451	0.03166	0.44809
15	0.08120	0.39936	0.17672	0.81384	0.45399	0.46651	2.14356	0.03443	0.44577
16	0.08720	0.39436	0.18919	0.80137	0.45549	0.47328	2.11290	0.03725	0.44342
17	0.09324	0.38936	0.20162	0.78893	0.45701	0.48018	2.08254	0.04012	0.44103
18	0.09929	0.38436	0.21401	0.77654	0.45856	0.48722	2.05246	0.04305	0.43861
19	0.10538	0.37936	0.22636	0.76418	0.46013	0.49440	2.02266	0.04604	0.43615
20	0.11149	0.37436	0.23867	0.75185	0.46172	0.50172	1.99315	0.04908	0.43365
21	0.11762	0.36936	0.25095	0.73957	0.46333	0.50919	1.96390	0.05218	0.43112
22	0.12378	0.36436	0.26318	0.72733	0.46498	0.51681	1.93493	0.05534	0.42855
23	0.12997	0.35936	0.27537	0.71513	0.46664	0.52460	1.90623	0.05856	0.42594
24	0.13619	0.35436	0.28752	0.70298	0.46833	0.53254	1.87779	0.06185	0.42330
25	0.14243	0.34936	0.29963	0.69086	0.47005	0.54066	1.84961	0.06520	0.42061
26	0.14870	0.34436	0.31170	0.67879	0.47180	0.54894	1.82168	0.06861	0.41788
27	0.15501	0.33936	0.32372	0.66676	0.47357	0.55741	1.79400	0.07210	0.41511
28	0.16134	0.33436	0.33569	0.65478	0.47537	0.56607	1.76657	0.07566	0.41230
29	0.16770	0.32936	0.34762	0.64284	0.47719	0.57491	1.73939	0.07929	0.40944
30	0.17409	0.32436	0.35951	0.63096	0.47905	0.58396	1.71244	0.08299	0.40654
31	0.18052	0.31936	0.37134	0.61911	0.48093	0.59321	1.68573	0.08677	0.40359
32	0.18697	0.31436	0.38313	0.60732	0.48284	0.60268	1.65925	0.09063	0.40060
33	0.19346	0.30936	0.39487	0.59557	0.48479	0.61237	1.63300	0.09457	0.39755
34	0.19998	0.30436	0.40656	0.58388	0.48676	0.62229	1.60698	0.09859	0.39446
35	0.20654	0.29936	0.41819	0.57223	0.48877	0.63244	1.58118	0.10270	0.39132
36	0.21313	0.29436	0.42978	0.56064	0.49080	0.64284	1.55559	0.10690	0.38813
37	0.21975	0.28936	0.44132	0.54910	0.49287	0.65350	1.53022	0.11120	0.38488
38	0.22641	0.28436	0.45280	0.53761	0.49498	0.66442	1.50507	0.11558	0.38158
39	0.23311	0.27936	0.46422	0.52618	0.49711	0.67562	1.48012	0.12007	0.37823
40	0.23984	0.27436	0.47560	0.51480	0.49928	0.68711	1.45537	0.12465	0.37482
41	0.24661	0.26936	0.48691	0.50347	0.50148	0.69890	1.43083	0.12934	0.37135
42	0.25341	0.26436	0.49818	0.49221	0.50372	0.71099	1.40649	0.13414	0.36782

	RESULTS SUMMARY - COMBINATION PATH										
	C2-OIL	C3-CO2	S (WATER)	S(OLEIC)	DIM VEL	DIM TIME	FWATR	FOIL	FCO2	C2BAR	C3BAR
1	0.50453	0.00000	0.49538	0.50462	2.93421	0.00000	0.85980	0.14020	0.00000	0.49316	0.15435
2	0.51353	0.00000	0.48620	0.51380	2.93421	0.01482	0.85980	0.14020	0.00000	0.49316	0.15435
3	0.52353	0.00000	0.47600	0.52400	2.93421	0.02964	0.85980	0.14020	0.00000	0.49316	0.15435
4	0.53353	0.00000	0.46579	0.53421	2.93421	0.04445	0.85980	0.14020	0.00000	0.49316	0.15435
5	0.54353	0.00000	0.45559	0.54441	2.93421	0.05927	0.85980	0.14020	0.00000	0.49316	0.15435
6	0.55353	0.00000	0.44539	0.55461	2.93421	0.07409	0.85980	0.14020	0.00000	0.49316	0.15435
7	0.56353	0.00000	0.43519	0.56481	2.93421	0.08891	0.85980	0.14020	0.00000	0.49316	0.15435
8	0.57353	0.00000	0.42499	0.57501	2.93421	0.10372	0.85980	0.14020	0.00000	0.49316	0.15435
9	0.58353	0.00000	0.41478	0.58522	2.93421	0.11854	0.85980	0.14020	0.00000	0.49316	0.15435
10	0.59353	0.00000	0.40458	0.59542	2.93421	0.13336	0.85980	0.14020	0.00000	0.49316	0.15435
11	0.60353	0.00000	0.39438	0.60562	2.93421	0.14818	0.85980	0.14020	0.00000	0.49316	0.15435
12	0.61353	0.00000	0.38418	0.61582	2.93421	0.16299	0.85980	0.14020	0.00000	0.49316	0.15435
13	0.62353	0.00000	0.37398	0.62602	2.93421	0.17781	0.85980	0.14020	0.00000	0.49316	0.15435
14	0.63353	0.00000	0.36377	0.63623	2.93421	0.19263	0.85980	0.14020	0.00000	0.49316	0.15435
15	0.64353	0.00000	0.35357	0.64643	2.93421	0.20745	0.85980	0.14020	0.00000	0.49316	0.15435
16	0.65353	0.00000	0.34337	0.65663	2.93421	0.22227	0.85980	0.14020	0.00000	0.49316	0.15435
17	0.66353	0.00000	0.33317	0.66683	2.93421	0.23708	0.85980	0.14020	0.00000	0.49316	0.15435
18	0.67353	0.00000	0.32296	0.67704	2.93421	0.25190	0.85980	0.14020	0.00000	0.49316	0.15435
19	0.68353	0.00000	0.31276	0.68724	2.93421	0.26672	0.85980	0.14020	0.00000	0.49316	0.15435
20	0.69353	0.00001	0.30256	0.69744	2.93421	0.28154	0.85980	0.14020	0.00000	0.49316	0.15435
21	0.70353	0.00019	0.29217	0.70783	2.93421	0.29635	0.85980	0.14020	0.00000	0.49316	0.15435
22	0.71353	0.00364	0.27853	0.72147	2.93421	0.31117	0.85980	0.14020	0.00000	0.49316	0.15435
23	0.71786	0.01352	0.26423	0.73577	2.93421	0.32599	0.85980	0.14020	0.00000	0.49316	0.15435
24	0.71695	0.01896	0.25973	0.74027	2.93421	0.34081	0.85980	0.14020	0.00000	0.49316	0.15435
25	0.71695	0.01896	0.25973	0.74027	2.93421	0.34081	0.26533	0.65664	0.07802	0.49316	0.15435
26	0.69569	0.01936	0.28105	0.71895	2.24566	0.37564	0.26533	0.65664	0.07802	0.40328	0.19626
27	0.67044	0.02436	0.30187	0.69813	2.24566	0.41047	0.26533	0.65664	0.07802	0.37804	0.20126
28	0.65345	0.02936	0.31427	0.68573	2.24566	0.44530	0.26533	0.65664	0.07802	0.36105	0.20626
29	0.63923	0.03436	0.32385	0.67615	2.13730	0.46788	0.28533	0.62576	0.08891	0.34645	0.21514
30	0.62643	0.03936	0.33199	0.66801	2.06485	0.48430	0.30168	0.59889	0.09943	0.33639	0.22139
31	0.61452	0.04436	0.33922	0.66078	1.99502	0.50125	0.31567	0.57474	0.10959	0.32643	0.22766
32	0.60324	0.04936	0.34582	0.65418	1.92864	0.51850	0.32797	0.55262	0.11941	0.31670	0.23388
33	0.59242	0.05436	0.35195	0.64805	1.86580	0.53596	0.33899	0.53211	0.12890	0.30723	0.24001
34	0.58197	0.05936	0.35771	0.64229	1.80637	0.55360	0.34897	0.51294	0.13809	0.29801	0.24603
35	0.57182	0.06436	0.36317	0.63683	1.75014	0.57138	0.35811	0.49491	0.14698	0.28904	0.25195
36	0.56192	0.06936	0.36838	0.63162	1.69689	0.58931	0.36653	0.47786	0.15561	0.28031	0.25775
37	0.55224	0.07436	0.37337	0.62663	1.64639	0.60739	0.37434	0.46169	0.16397	0.27182	0.26345
38	0.54275	0.07936	0.37817	0.62183	1.59845	0.62561	0.38161	0.44630	0.17209	0.26354	0.26904
39	0.53343	0.08436	0.38281	0.61719	1.55288	0.64396	0.38841	0.43162	0.17997	0.25548	0.27453
40	0.52426	0.08936	0.38730	0.61270	1.50952	0.66246	0.39479	0.41758	0.18763	0.24762	0.27992
41	0.51522	0.09436	0.39166	0.60834	1.46820	0.68110	0.40078	0.40414	0.19508	0.23996	0.28521
42	0.50631	0.09936	0.39589	0.60411	1.42880	0.69989	0.40643	0.39124	0.20233	0.23249	0.29040
43	0.49752	0.10436	0.40001	0.59999	1.39117	0.71882	0.41177	0.37885	0.20938	0.22519	0.29550

SHOCK DETERMINATION

K	DIFF	C2F	DVF	CSL2	CSL3	DIF3
2	2.18264	0.51353	2.18264	0	0	2.18264
3	-0.55633	0.52353	2.37787	2.93421	0	2.37787
4	-0.3647	0.53353	2.56951	2.93421	0	2.56951
5	-0.18024	0.54353	2.75397	2.93421	0	2.75397
6	-0.00667	0.55353	2.92754	2.93421	0	2.92754
7	0.15225	0.56353	3.08646	2.93421	0	3.08646
8	0.29289	0.57353	3.22709	2.93421	0	3.22709
9	0.41191	0.58353	3.34612	2.93421	0	3.34612
10	0.50644	0.59353	3.44065	2.93421	0	3.44065
11	0.5742	0.60353	3.50841	2.93421	0	3.50841
12	0.61363	0.61353	3.54784	2.93421	0	3.54784
13	0.62397	0.62353	3.55817	2.93421	0	3.55817
14	0.60528	0.63353	3.53949	2.93421	0	3.53949
15	0.55846	0.64353	3.49267	2.93421	0	3.49267
16	0.48514	0.65353	3.41935	2.93421	0	3.41935
17	0.38759	0.66353	3.3218	2.93421	0	3.3218
18	0.26861	0.67353	3.20282	2.93421	0	3.20282
19	0.13136	0.68353	3.06557	2.93421	0	3.06557
20	-0.02061	0.69353	2.9136	2.93421	0	2.9136
21	-0.07187	0.70353	2.86234	2.93421	2.86123	0.00111
22	0.01415	0.71353	2.94836	2.93421	2.91961	0.02875
23	0.01566	0.71786	2.94987	2.93421	2.94931	0.00056
24	-0.81622	0.71695	2.11799	2.93421	2.8819	-0.76391
25	-1.14383	0.73072	1.88076	3.02459	2.87396	-0.9932
26	-1.66439	0.47752	2.20563	3.87002	3.26127	-1.05564
27	-1.77908	0.47314	2.09094	3.87002	3.2064	-1.11546
28	-1.89004	0.46903	1.97998	3.87002	3.15137	-1.17139
29	-1.99706	0.46524	1.87296	3.87002	3.09639	-1.22343
30	-2.10006	0.46187	1.76996	3.87002	3.04161	-1.27165
31	-2.19908	0.459	1.67094	3.87002	2.98717	-1.31623

SHOCK LOCATED IN COMBINED PATH:		
PEAK OF F2F VS C2F	24	IC2M
STARTING LOCATION OF SHOCK	1	M
ENDING LOCATION OF SHOCK	24	MS
CO2 CONCENTRATION AT START	0.01936	FRACTN
OIL CONCENTRATION AT START	0.69569	FRACTN
OIL CONCENTRATION AT END OF SHOCK	0.65345	FRACTN
CO2 CONCENTRATION AT END OF SHOCK	0.02936	FRACTN
CORD SLOPE OF SHOCK DELF2/DELC2	2.24566	
CORD SLOPE OF SHOCK DELF3/DELC3	2.8819	

KOVAL "H" FACTOR(FUNCTION OF VDP)	1	HETR	
KOVAL "E" FACTOR (1/4 POWER RULE)	2.6979	E	
KOVAL K-FACTOR	2.6979	YK	YK
PORE VOLUME	2717.6	UTVP	M.BBL
ORIGINAL HYDROCARBON PORE VOLUME	2500.2	UOHPV	M.RB
INITIAL HYDROCARBON PORE VOLUME	1371.4	UTHPV	M.RB
INITIAL OIL IN PLACE	1124.1	UIOIP	M.STB

1D SUMMARY

DIM TIM		HCPV		PRODUCING RATES			CUMULATIVE			CUMULATIVE		OIL
TIME YEARS	TIME PV	CO2	WATER	OIL STB/D	CO2 MCF/D	WATER STB/D	OIL MSTB	CO2 MMCF	WATER MSTB	WATER MSTB	CO2 MMCF	RECV FR OIP
0.00	0.00	0	0	44.818	0.0007	335.32	0	0	0	0	0	0
0.28	0.01	0.0081	0.0081	44.818	0.0007	335.32	4.6276	7E-05	34.623	20.135	45.79117132	0.0041
0.57	0.03	0.0161	0.0161	44.818	0.0007	335.32	9.2552	0.0001	69.247	40.269	91.58234264	0.0082
0.85	0.04	0.0242	0.0242	44.818	0.0007	335.32	13.883	0.0002	103.87	60.404	137.373514	0.0124
1.13	0.06	0.0322	0.0322	44.818	0.0007	335.32	18.51	0.0003	138.49	80.538	183.1646853	0.0165
1.41	0.07	0.0403	0.0403	44.818	0.0007	335.32	23.138	0.0004	173.12	100.67	228.9558566	0.0206
1.70	0.09	0.0483	0.0483	44.818	0.0007	335.32	27.766	0.0004	207.74	120.81	274.7470279	0.0247
1.98	0.10	0.0564	0.0564	44.818	0.0007	335.32	32.393	0.0005	242.36	140.94	320.5381992	0.0288
2.26	0.12	0.0644	0.0644	44.818	0.0007	335.32	37.021	0.0006	276.99	161.08	366.3293706	0.0329
2.55	0.13	0.0725	0.0725	44.818	0.0007	335.32	41.649	0.0006	311.61	181.21	412.1205419	0.0371
2.83	0.15	0.0805	0.0805	44.818	0.0007	335.32	46.276	0.0007	346.23	201.35	457.9117132	0.0412
3.11	0.16	0.0886	0.0886	44.818	0.0007	335.32	50.904	0.0008	380.86	221.48	503.7028845	0.0453
3.39	0.18	0.0966	0.0966	44.818	0.0007	335.32	55.531	0.0009	415.48	241.61	549.4940558	0.0494
3.68	0.19	0.1047	0.1047	44.818	0.0007	335.32	60.159	0.0009	450.1	261.75	595.2852272	0.0535
3.96	0.21	0.1127	0.1127	44.818	0.0007	335.32	64.787	0.001	484.73	281.88	641.0763985	0.0576
4.24	0.22	0.1208	0.1208	44.818	0.0007	335.32	69.414	0.0011	519.35	302.02	686.8675698	0.0618
4.53	0.24	0.1288	0.1288	44.818	0.0007	335.32	74.042	0.0011	553.97	322.15	732.6587411	0.0659
4.81	0.25	0.1369	0.1369	44.818	0.0007	335.32	78.67	0.0012	588.6	342.29	778.4499124	0.07
5.09	0.27	0.145	0.145	44.818	0.0007	335.32	83.297	0.0013	623.22	362.42	824.2410838	0.0741
5.37	0.28	0.153	0.153	44.818	0.0007	335.32	87.925	0.0013	657.84	382.56	870.0322551	0.0782
5.66	0.30	0.1611	0.1611	44.818	0.0007	335.32	92.552	0.0014	692.47	402.69	915.8234264	0.0823
5.94	0.31	0.1691	0.1691	44.818	0.0007	335.32	97.18	0.0015	727.09	422.82	961.6145977	0.0865
6.22	0.33	0.1772	0.1772	44.818	0.0007	335.32	101.81	0.0016	761.71	442.96	1007.405769	0.0906
6.51	0.34	0.1852	0.1852	44.818	0.0007	335.32	106.44	0.0016	796.34	463.09	1053.19694	0.0947
6.51	0.34	0.1852	0.1852	209.91	69.204	103.48	106.44	0.0016	796.34	463.09	1053.19694	0.0947
6.54	0.34	0.1862	0.1862	209.91	69.204	103.48	108.98	0.8415	797.59	465.46	1058.579004	0.097
6.57	0.34	0.1871	0.1871	209.91	69.204	103.48	111.53	1.6813	798.85	467.83	1063.961067	0.0992
6.61	0.35	0.1881	0.1881	209.91	69.204	103.48	114.08	2.5212	800.1	470.19	1069.343131	0.1015
6.64	0.35	0.189	0.189	209.91	69.204	103.48	116.63	3.3611	801.36	472.56	1074.725194	0.1038
6.67	0.35	0.19	0.19	209.91	69.204	103.48	119.17	4.2009	802.62	474.93	1080.107258	0.106
6.71	0.35	0.1909	0.1909	209.91	69.204	103.48	121.72	5.0408	803.87	477.29	1085.489321	0.1083
6.74	0.35	0.1918	0.1918	209.91	69.204	103.48	124.27	5.8806	805.13	479.66	1090.871384	0.1106
6.77	0.35	0.1928	0.1928	209.91	69.204	103.48	126.82	6.7205	806.38	482.03	1096.253448	0.1128
6.81	0.36	0.1937	0.1937	209.91	69.204	103.48	129.36	7.5603	807.64	484.39	1101.635511	0.1151
6.84	0.36	0.1947	0.1947	209.91	69.204	103.48	131.91	8.4002	808.89	486.76	1107.017575	0.1174
6.87	0.36	0.1956	0.1956	209.91	69.204	103.48	134.46	9.24	810.15	489.13	1112.399638	0.1196
6.91	0.36	0.1966	0.1966	209.91	69.204	103.48	137	10.08	811.41	491.49	1117.781702	0.1219
6.94	0.36	0.1975	0.1975	209.91	69.204	103.48	139.55	10.92	812.66	493.86	1123.163765	0.1241
6.97	0.37	0.1985	0.1985	209.91	69.204	103.48	142.1	11.76	813.92	496.23	1128.545828	0.1264
7.01	0.37	0.1994	0.1994	209.91	69.204	103.48	144.65	12.599	815.17	498.59	1133.927892	0.1287
7.04	0.37	0.2004	0.2004	209.91	69.204	103.48	147.19	13.439	816.43	500.96	1139.309955	0.1309
7.07	0.37	0.2013	0.2013	209.91	69.204	103.48	149.74	14.279	817.69	503.32	1144.692019	0.1332
7.10	0.37	0.2023	0.2023	209.91	69.204	103.48	152.29	15.119	818.94	505.69	1150.074082	0.1355
7.14	0.37	0.2032	0.2032	209.91	69.204	103.48	154.84	15.959	820.2	508.06	1155.456146	0.1377
7.17	0.38	0.2042	0.2042	209.91	69.204	103.48	157.38	16.799	821.45	510.42	1160.838209	0.14
7.17	0.38	0.2042	0.2042	209.91	69.204	103.48	157.38	16.799	821.45	510.42	1160.838209	0.14
7.84	0.41	0.2231	0.2231	209.91	69.204	103.48	208.33	33.596	846.57	557.75	1268.479478	0.1853
8.50	0.45	0.242	0.242	209.91	69.204	103.48	259.28	50.393	871.69	605.08	1376.120746	0.2307
8.93	0.47	0.2543	0.2543	200.04	78.861	111.28	290.75	62.799	889.19	635.76	1445.889913	0.2587
9.25	0.48	0.2632	0.2632	191.45	88.191	117.66	312.65	72.888	902.65	658.07	1496.622982	0.2781
9.57	0.50	0.2724	0.2724	183.73	97.202	123.11	334.36	84.369	917.19	681.1	1549.004993	0.2975
9.90	0.52	0.2818	0.2818	176.66	105.91	127.91	355.59	97.102	932.57	704.54	1602.318893	0.3163
10.23	0.54	0.2913	0.2913	170.1	114.33	132.2	376.29	111.01	948.66	728.27	1656.282645	0.3348
10.57	0.55	0.3009	0.3009	163.97	122.48	136.1	396.44	126.06	965.38	752.23	1710.774973	0.3527
10.91	0.57	0.3105	0.3105	158.21	130.37	139.66	416.05	142.22	982.69	776.4	1765.741521	0.3701
11.25	0.59	0.3203	0.3203	152.76	138.02	142.95	435.14	159.47	1000.6	800.77	1821.15803	0.3871
11.60	0.61	0.3301	0.3301	147.59	145.44	145.99	453.73	177.79	1018.9	825.33	1877.01444	0.4036
11.94	0.63	0.34	0.34	142.67	152.63	148.83	471.83	197.16	1037.8	850.08	1933.307537	0.4198
12.29	0.64	0.35	0.35	137.98	159.63	151.48	489.48	217.58	1057.2	875.03	1990.037401	0.4355
12.65	0.66	0.36	0.36	133.49	166.42	153.97	506.69	239.03	1077.1	900.16	2047.205631	0.4508
13.00	0.68	0.3702	0.3702	129.19	173.03	156.3	523.48	261.51	1097.4	925.49	2104.81446	0.4657
13.36	0.70	0.3804	0.3804	125.07	179.45	158.51	539.85	285	1118.1	951.02	2162.866319	0.4803
13.72	0.72	0.3907	0.3907	121.11	185.71	160.59	555.82	309.5	1139.3	976.74	2221.363639	0.4945
14.09	0.74	0.401	0.401	117.3	191.8	162.56	571.41	334.99	1160.9	1002.7	2280.308766	0.5083
14.45	0.76	0.4115	0.4115	113.62	197.74	164.43	586.63	361.47	1182.9	1028.8	2339.703956	0.5219
14.82	0.78	0.422	0.422	110.08	203.53	166.2	601.48	388.94	1205.4	1055.1	2399.551395	0.5351
15.20	0.80	0.4326	0.4326	106.67	209.18	167.89	615.99	417.38	1228.2	1081.6	2459.853231	0.548
15.57	0.82	0.4433	0.4433	103.37	214.68	169.49	630.15	446.79	1251.4	1108.3	2520.611619	0.5606
15.95	0.84	0.4541	0.4541	100.18	220.06	171.02	643.98	477.17	1275	1135.2	2581.828763	0.5729
16.33	0.86	0.4649	0.4649	97.095	225.31	172.47	657.48	508.51	1299	1162.4	2643.506954	0.5849
16.71	0.88	0.4758	0.4758	94.109	230.44	173.86	670.67	540.79	1323.4	1189.7	2705.64861	0.5966
17.10	0.90	0.4868	0.4868	91.216	235.45	175.19	683.55	574.03	1348.1	1217.2	2768.256305	0.6081
17.49	0.92	0.4979	0.4979	88.411	240.35	176.46	696.12	608.22	1373.2	1244.9	2831.332796	0.6193
17.88	0.94	0.5091	0.5091	85.692	245.14	177.67	708.4	643.35	1398.6	1272.9	2894.881053	0.6302
18.28	0.96	0.5204	0.5204	83.052	249.83	178.83	720.39	679.41	1424.5	1301	2958.904274	0.6409
18.68	0.98	0.5317	0.5317	80.49	254.41	179.94	732.1	716.41	1450.6	1329.4	3023.405905	0.6513
19.08	1.00	0.5431	0.5431	78.002	258.9	181	743.53	754.35	1477.2	1358	3088.389653	0.6615